Virtual Lab for Fibre Reinforced Concrete Design by Simulation Prototyping

FibreLAB

Project funded by the European Community under the Eurostars project E!10316

D5.1 Example & Validation Manual

Responsible author: Peter K. Juhasz

Co-authors:

Peter Schaul, Zdeněk Janda, J. Cervenka

Status: final
Type: software/pilot
Access: public
Version: 3.0
Date: 16. 7. 2019

Project website:
http://www.fibrelab.eu

Executive summary:

This is the FibreLAB project document. This document is being continuously updated during the project. The report describes the examples and validation of software tools developed during the FibreLAB project. This work is part of workpackage W5 - Validation. This work package evaluates the developed software from three points of view: accuracy and relevance to the real behaviour of fibre reinforced material, robustness and efficiency and user-friendliness, ease if use.

The accuracy and predictive capacity of the software will be evaluated using the existing experiments of the partners or the experimental data available in the literature. CER previously participated in various projects involving numerical analysis of experimental data. JKP has a close and long term cooperation with the Budapest University of Technology and its experimental laboratory: Czako Adolf Laboratory (Department of Mechanics, Materials & Structures). This provides a large database of cca 20-50 experimental data that can be used to the software validation.

Important criterion for success of the project is the robustness and efficiency of the developed software. If it is to be used and accepted in the engineering practice it needs to provide accurate results, but the results have to provided also very quickly almost in real time.

The software should perform the requested analysis in terms of minutes with the upper limit of 2-3 hours for more advanced calculation types.

User friendliness and ease of use is also an important parameter, which will be evaluated in this package mainly by engineers from JKP, which understand the needs of the practice, and have extensive experience from using other design software products.

Based in the validation and evaluation process, the final adjustment of the software will be performed before the completion of the project.

The project develops software tools to support the design of advanced structures or products from fibre reinforced concrete (FRC) using simulation prototyping. The software will support engineers during the design process, which will be based on the simulation of the structural performance during the foreseen design scenarios for the individual design limit states: serviceability and ultimate limit states as well as the new design states such as: robustness, durability and service life verification.

The software will be developed based on the existing product ATENA developed and distributed by CER. The project will develop a separate module of this system specifically targeted for fibre reinforced concrete industry.

This product can be used separately or together with the existing ATENA software. The product shall also support parametric modelling and embedded scripting language to enable the fast development of even more specialized design tools for the development and design of specific construction products for precast industry or other mass production.

Revision history:

date	author	status	changes
16. 05. 2019	J. Červenka	1.0	Draft document version prepared
11. 07. 2019	P. K. Juhász	2.0	Semi-final version prepared
17. 07. 2019	J. Červenka	3.0	Final editing of version 3.0 before official release

Table of contents:

1. General

In this work package methods and software tools that have been developed in workpackages WP2, WP3 and WP4 are evaluated and tested on experimental data and practical engineering projects. This work is divided into the following tasks:

Task 5.1: Validation - the developed software tools will be validated and evaluated in terms of their accuracy and predictive capacity using the existing experiments of the partners or the experimental data available in the literature. CER previously participated in various projects involving numerical analysis of experimental data. JKP has a close and long term cooperation with the Budapest University of Technology and its experimental laboratory: Czako Adolf Laboratory (Department of Mechanics, Materials & Structures). This provides a large database of cca 20-50 experimental data that can be used to the software validation. The validation process will concentrate also on efficiency and ease of use. The results of this validation task will be summarized in the deliverable D5.1.

It should be noted that first ad-hoc initial testing will be performed continuously during the product development in WP2, WP3 and WP4. Task 5.1 represents a comprehensive testing program based on the requirements specified in WP1 and D1.1.

Task 5.2: Software adjustment based on the validation process - it was expected that the validation process would discover some weaknesses of problems in the developed software tools or methods. This task should give few man-months for the software developer to make final adjustments and improvements before the project end and the commercialization and exploitation of the project products.

Task 5.3: Final software validation & evaluation - this task involved the final testing and evaluation process, which verified whether the identified problems and proposed mitigation actions from Task 5.1 had been properly addressed in Task 5.2.

2. Identification of Material Parameters

Determination of appropriate material parameters for the fibre reinforced concrete material model [28] in design and assessment of structures is an important task, which is necessary for realistic modelling of FRC structures.

There are many guidelines to model and design fibre reinforced concrete, such as RILEM TC162-TDF[31], *fib* Model Code 2010 [15], ÖVBB Richtlinie Faserbeton [22], ACI 544.8R-16 [1], CNR DT[12]. All of these guidelines are based on a three or four point bending tests. Obtained test results as load-displacement or load-CMOD diagrams are converted to the parameters that can be used as a material model. RILEM and *fib* Model Code 2010 use residual strengths and define "stress-crack width" or "stress-strain" diagrams that can be applied as material laws. ACI describes an indirect method to obtain the stress-strain response.

In finite element model the stress-strain diagram can be used if the characteristic length and the direction of the principal stress is known. In this case, the stress-strain can be converted to stress-crack width and the crack localization can be handled. For this purpose, the crack band size method can be used [2].

These stress-strain models based on guidelines can be applied if the Bernoulli-Navier hypothesis is valid (and as a consequence there is a linear elastic stress distribution in the cross section). However, in reality, the stress distribution will be different due to the notch that is usually in the middle of the specimen for three point bending test or due to the cracks in the material that are formed during the test.

In this case, it is necessary to obtain material laws for finite element analysis by different method. As was shown in papers [25] and [27] material parameters can be determined by inverse analysis of results from basic tests as three of four point bending. Another method was proposed by Juhász [16], and it works with fracture energy of material composed of concrete matrix and fibres. It is reasonable to model the FRC with "stress-crack width", instead of "stress-strain" diagram. The shape of the softening curve after post crack can depend on the type of the fibre and the dosage, but most of the time it can be simplified as a constant value after crack (so called residual strength). The area under the "stress-crack width" diagram is the fracture energy. This fracture energy could be divided into 2 parts: fracture energy of the concrete matrix G_F and added fracture energy of fibres G_{Ff}, see Figure 1. These two methods are discussed in this chapter and compared with material laws obtained by guidelines.

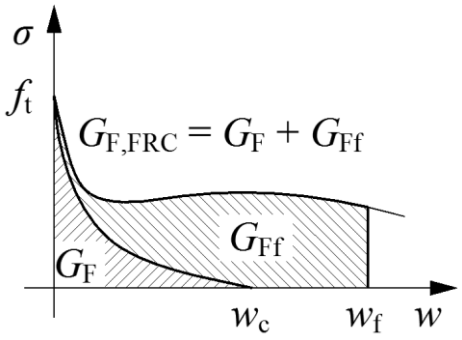

Figure 1: Fracture energy of the concrete and added fracture energy by the fibres

2.1 Finite Element Analysis

Behaviour of FRC material is analysed in program ATENA [28] for non-linear analysis of concrete structures. ATENA is capable of a realistic simulation of concrete behaviour in the entire loading range with ductile as well as brittle failure modes as shown for instance in [6]. It is based on the finite element

method and non-linear material models for concrete, reinforcement and their interaction. The tensile behaviour of concrete is described by smeared cracks, crack band and fracture energy and the compressive behaviour of concrete by a plasticity model with hardening and softening. The constitutive model is described in detail in [5]. Nonlinear solution is performed incrementally with equilibrium iterations in each load step.

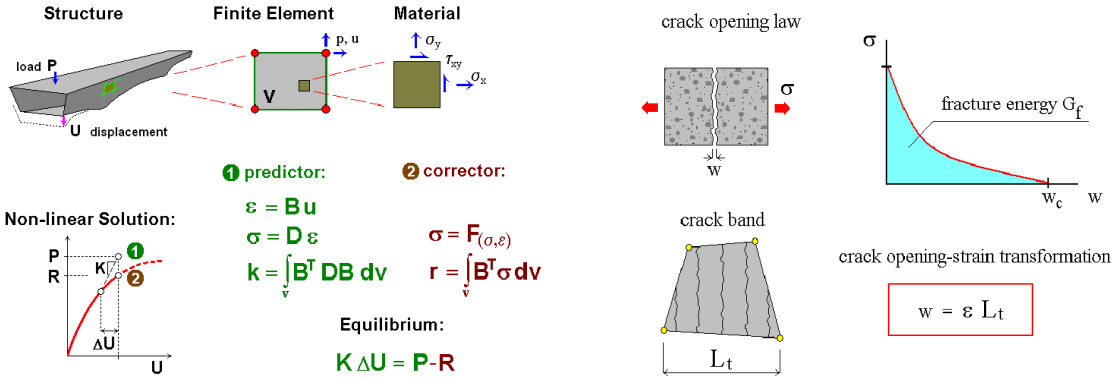

(a) (b)

Figure 2: (a) Scheme of the nonlinear finite element method, (b) smeared crack model for tensile behaviour of concrete

2.2 FRC Material Models

The tensile response of FRC differs from normal concrete not only in the values like tensile strength and especially fracture energy, but also in the shape of tensile softening branch. The original exponential function valid for normal concrete can be used as a first approach, but preferably would be to use more realistic form of the tensile constitutive law. Therefore, special material models at macroscopic level are needed for modelling of fibre reinforced concrete.

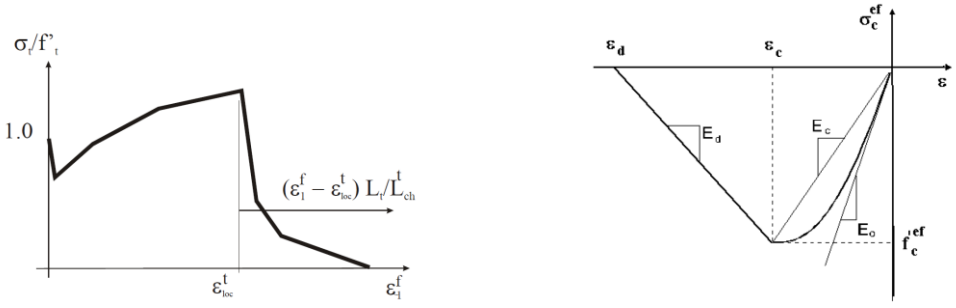

(a) (b)

Figure 3: (a) User defined tensile behaviour, (b) compressive stress-strain law

The most sophisticated and most general model of FRC material represents an extension to the fracture-plastic constitutive law [5] called 3D NLC2 User model. It describes the tensile behaviour according to the material response measured in tests point-wise in terms of the stress-strain relationship. The first part of the diagram is the usual stress-strain constitutive law. After exceeding the localization strain ε_{loc} the material law assumed for the characteristic crack band width L_{ch} is adjusted to the actual crack band width L_t. The characteristic crack band width (characteristic length) is the size (length) for which the defined material law is valid. The same procedure (with eventually different characteristic length) is

used for the compression part of the material law. Compressive stress-strain law of mentioned material models is described in Figure 3. The softening law in compression is linearly descending and the end point of the softening curve is defined by plastic displacement w_d (corresponding to ε_d in Figure 3b). By increasing material parameter w_d the contribution of the fibres to the compressive behaviour of concrete is considered. Another important compressive parameter for FRC modelling is reduction of compressive strength due to cracks which says how the strength is reduced while the material is subjected to lateral tension.

2.3 Experimental Validation

Experimental program focused on application of synthetic fibres called BarChip48 in concrete C25/30 is chosen for the presented study. Different dosages of fibres were tested as is shown in load-displacement diagrams in Figure 4b. Six tests were provided for each dosage, the plotted curves represent mean values. Geometry of the specimen and test setup corresponds to EN 14651 [14]. Beams were tested under three point bending condition. The cross section is 150x150 mm and span is 500 mm. The central part of the beam is weakened by notch 25 mm long, see Figure 4a.

Result for fibre dosage 2 kg/m^3 was chosen for numerical analysis presented in this chapter.

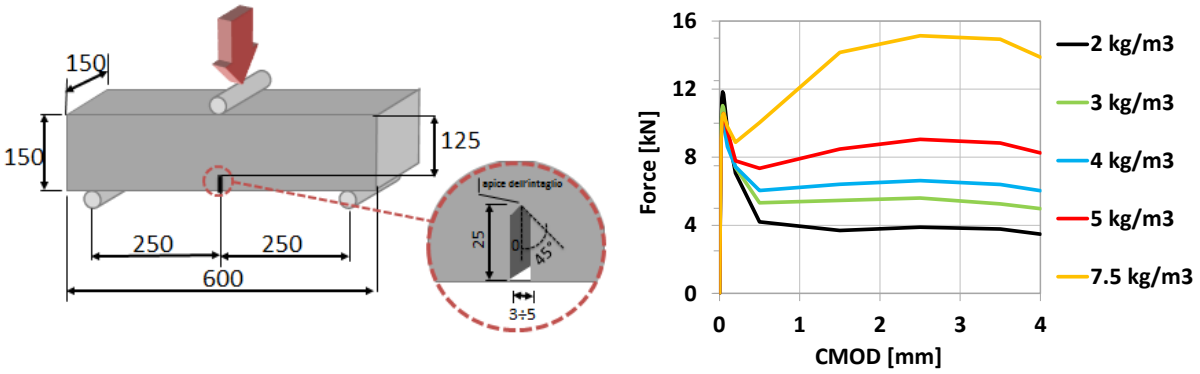

(a) (b)

Figure 4: (a) Geometry of tested specimen, (b) comparison of LD diagrams for different fibre dosages

2.4 Material Law for Fibre Reinforced Concrete

2.4.1 Recommendations from Guidelines

As a representative document, RILEM TC162-TDF is chosen for determination of the material law. Experimental programme described in previous chapter involves the same test procedure and specimen geometry that is described in RILEM. Flexural tensile strengths $f_{R,i}$ are determined Based on Bernoulli-Navier hypothesis by expression:

$$f_{R,i} = \frac{3F_{R,i}L}{2bh_{sp}^2} \tag{1}$$

where b is width of the specimen,
h_{sp} is distance between tip of the notch and top of cross section,
L is span of the specimen,
$F_{R,i}$ is load recorded at CMOD$_i$.

Maximal flexural strength $f_{fctm,fl}$ and residual flexural strengths for crack mouth opening displacement *CMOD* 0.5 mm ($f_{R,1}$) and 3.5 mm ($f_{R,4}$) are used for the determination of material law, see Figure 5 left. Stress-strain diagram defined by RILEM is trilinear, for the numerical model part after the peak is important. Final diagram utilized in the numerical analysis contains bilinear softening as is shown in Figure 5 right.

The finite element model for bending test is made for a plane stress simplification, with low order quadrilateral elements with 2x2 integration scheme, with the square elements shape and size of 5 mm, i.e. 30 elements through the height (25 elements above notch), see Figure 6a. The loading is applied by force on the top loading plate. *CMOD* is calculated as difference between horizontal displacement of the right and left bottom part of the notch. Characteristic length for tensile stress-strain diagram is equal to the element size, i.e. 5 mm.

Comparison of the load-displacement diagram from test and numerical simulation is shown in Figure 6b. Model can correctly describe behavior on the tail of the diagram but there are differences after the crack localization. Model according to RILEM underestimate the flexural strength of the material.

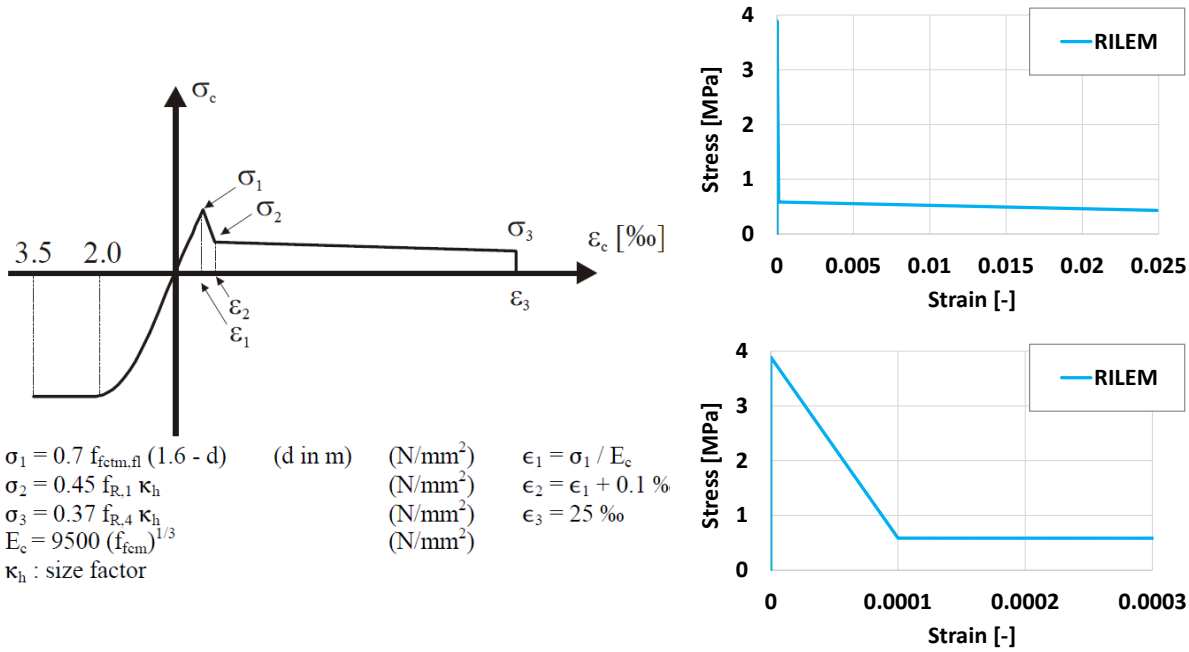

Figure 5: (left) Stress-strain diagram according to RILEM TC162-TDF [31], (right top) diagram for material with fibre dosage 2 kg/m^3, (right bottom) detail of the diagram until strain 0.0003

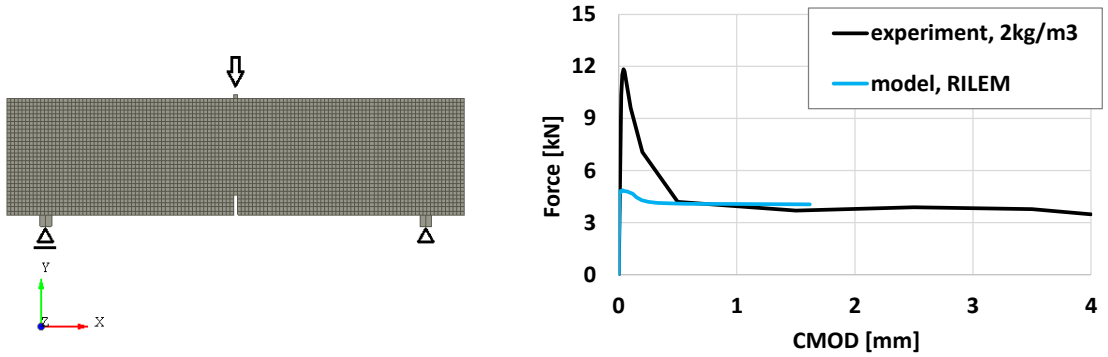

(a) (b)

Figure 6: (a) FEM model of three point bending test, (b) comparison of experimental result for fibre dosage 2 kg/m^3 and model with RILEM material law (characteristic length 5 mm)

2.4.2 Inverse Analysis

Another way how to obtain FRC material law for nonlinear finite element analysis is inverse analysis of experimental results which consists of two main steps. The first one is the estimation of material law based on mixture, contents and type of fibres, etc. or guidelines recommendations. The second step is modification of initial law by inverse analysis of material tests, mainly four-point bending test until the required accuracy of results is achieved.

In this case, RILEM material law was utilized as an initial function and by several simulations it was modified to the optimal material law for investigated FRC that is shown in Figure 7a. It is obvious that material law is described in more detail compared to the RILEM and it leads to more accurate behaviour during bending test, see Figure 7b.

Advantage of this approach is that it can be used for any experimental result and specimen geometry and it is possible to describe material very precisely. As a disadvantage, more than one numerical simulation are necessary for satisfactory result. For example, presented result was found by performing three analyses. For automated inverse analysis, it is possible to use program FraMePID-3PB [20].

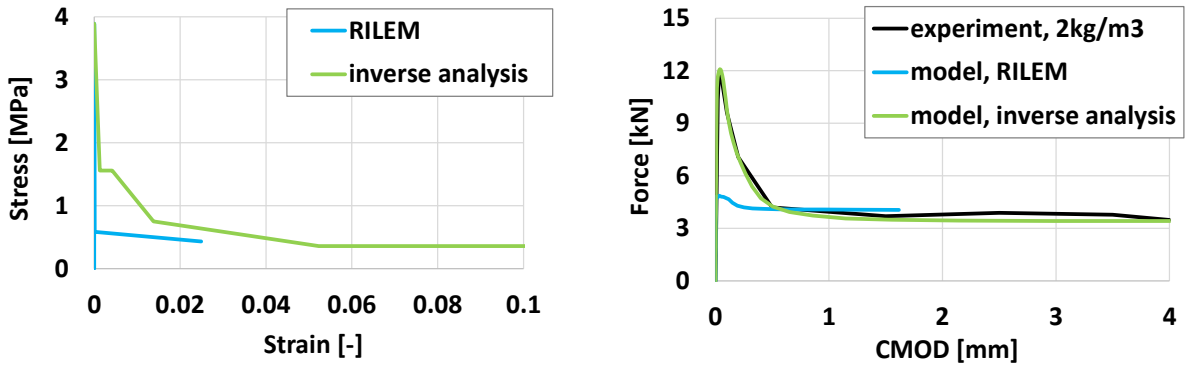

(a) (b)

Figure 7: (a) Stress-strain from inverse analysis in comparison with RILEM, (b) comparison of experimental result for fibre dosage 2 kg/m^3 and model with RILEM material law and law obtained by inverse analysis

2.4.3 Modified Fracture Energy Method

The third method was proposed by Juhász [16], and it utilizes the fracture energy of the FRC.

Fracture energy of concrete can be estimated by many recommendations. Although the added fibre increases fracture energy, only a few instances occur when fibre reinforced concrete is modelled by considering modification of fracture energy, however it would be plausible. Added fibres increase this residual strength and the ductility of the material, thus increasing fracture energy of concrete. The various types of fibres exert their primary effect at different crack width [16]. Steel fibres with higher elastic modulus are able to take high stress even at low crack width, however by the increase of crack width fibres tear or pull out from the matrix, thus resulting in the decrease of residual stress. However, synthetic fibres of low elastic modulus can work even at higher strain than steel fibres, meaning that synthetic fibres behave efficiently in the case of higher crack width.

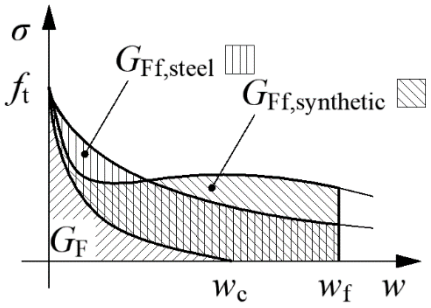

Figure 8: σ-w diagram of steel- and synthetic fibre reinforced concrete and interpretation of fracture energy

Crack width at which stress terminates between the crack surfaces of the concrete is called final crack opening width marked by w_c. In the case of fibre reinforced concrete this value is significantly higher, so it can be taken into account during calculation with a given value, according to guidelines. Thus, considered maximum crack opening width of fibre reinforced concrete is marked by w_f. Value of w_f depends on the type and length of the fibre, its recommended baseline value is w_f =3 mm. Fracture energy of the concrete is the area below the stress-crack width diagram of the concrete, marked by G_F, while for fibre reinforced concrete it is similarly the area below its curve, marked by G_{FFRC}. Fracture energy added by fibres is the difference of the two, thus: $G_{Ff} = G_{FFRC} - G_F$ (Figure 9).

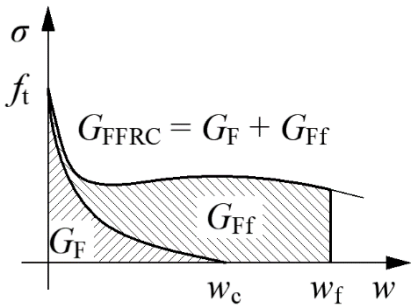

Figure 9: Fracture energy of concrete and fibre reinforced concrete, and added fracture energy

Based on both my own experimental results and the publications found in the literature it can be stated that post-cracking residual strength of synthetic fibres takes an approximately constant value. A simplified constitutive law is usually provided in the guidelines, where post-cracking tension strength is

modelled by a constant value (fib, 2012; ÖVBB, 2013). Based on the fib model code 2010 value of the post-cracking tension strength in the case of rigid-plastic model is the following:

$$f_{Ftu} = \frac{f_{R3}}{3} \tag{2}$$

where f_{Ftu} is thepost-cracking residual tension strength,
f_{R3} is the residual flexural tensile strength corresponding to CMOD = 3 mm, according to eq (1).

From the above the following constitutive law can be defined according to Figure 10. Value of f_f can be defined based on the guidelines, thus $f_f = f_{Ftu}$ based on the fib model code demonstrated above. The overlapping part of the G_F and G_{Ff} at the numerical diagram is negligible.

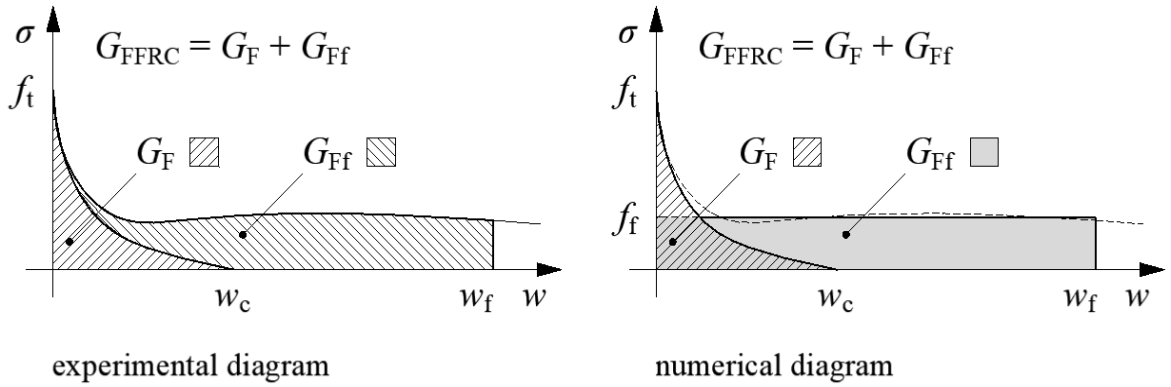

Figure 10: Experimental and numerical diagram of fibre reinforced concrete

Based on the above model added fracture energy (G_{Ff}) can be defined as follows:

$$G_{Ff} = f_f \, w_f \tag{3}$$

3. Example 1 - Layered FRC Structural Elements

As an example of procedure of FRC modelling by nonlinear finite element method, layered FRC elements were chosen [29]. Layered FRC elements are created from two or more layers of material with continuously variable composition and microstructure. Since the fibres are one of the most expensive components of the composite the aim is to use them as efficiently as possible and thereby reduce the amount of fibres and cost of materials at the same time. The principle consists in gradually changing the material composition and microstructure over a structural element volume so that the local properties meet the local load-resisting requirements.

The layered structural elements can be used for façade panels, floor structures in buildings (for new buildings as well as for reconstruction), for bridge structures or impact and blast resistant elements. In this chapter, the layered element consisting of five layers and designed to sustain bending moment is presented.

3.1 Identification of FRC Parameters

The FRC input parameters must be determined for material corresponding to the class C110/130. Concrete matrix is reinforced with the steel fibres in volume fraction 1.5 %. Experimental verification of cylinder compressive strength after 28 days is 125 MPa, Young's modulus is 45 GPa. Identification of FRC parameters is based on the results of four-point bending tests, see Figure 11.

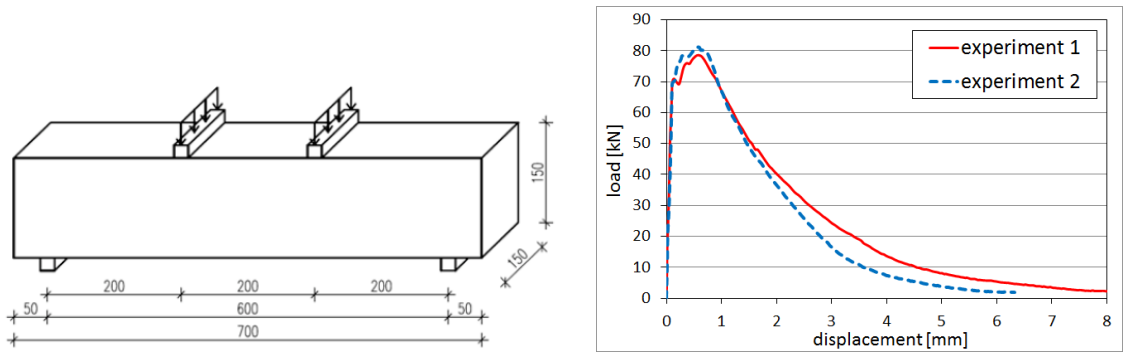

(a) (b)

Figure 11: (a) Scheme of four-point bending test, (b) Experimental results

For the inverse analysis, stochastic approach can be used (randomization of initial material input parameters by probabilistic system SARA, numerical reproduction of four-point bending tests, comparison with experimental results and selection of appropriate parameters). Another approach is software Consoft developed by prof. Dr.-Ing. Volker Slowik and his colleagues at the University of Applied Sciences in Leipzig, Germany [13]. Automatic analysis based on the evolutionary algorithms is used for the determination of cohesive law function. The second approach was applied in this study.

The best results of inverse analysis are shown in Figure . Softening curves for two material models are shown in the Figure 12 (a), comparison between numerical and experimental results is shown in the Figure 12 (b). The results of numerical simulations are in a perfect accordance with the experimental results.

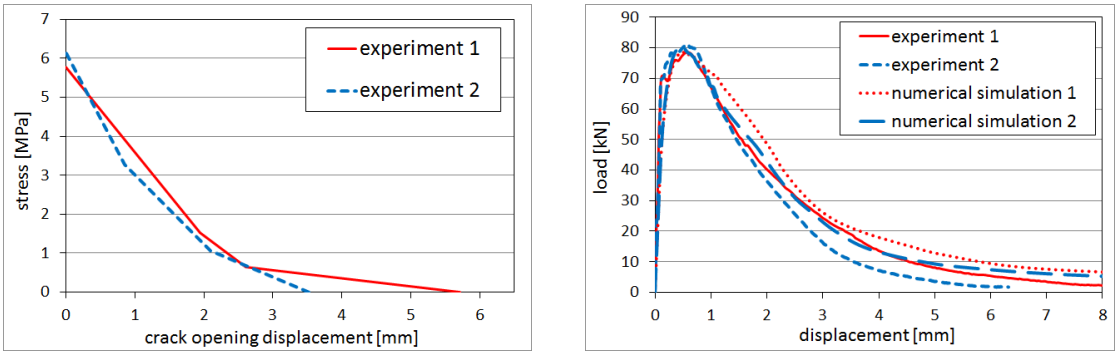

(a) (b)

Figure 12: (a) Softening curves, (b) Comparison of experimental results and numerical simulations of four-point bending tests

3.2 Validation of Modified Material Model

Material model 3D NLC2 User with softening curve derived in the previous chapter was validated by the numerical simulation of bridge slabs used for reconstruction of a bridge in Czech Republic; they should serve as a permanent formwork [18]. Slabs are made from the same material as was described in the previous chapter. Four-point bending tests of these slabs were carried out as shown in Figure 13 (a) – photo from the lab of the Klokner Institute of CTU. The dimensions of the slab are 1 x 1.67 m, the thickness is 20 mm, the rib thickness is 60 mm and thickness of the central rib is 40 mm. Load bearing capacity of the model was 20.6 kN which is pretty close to the experiment. The failure (fracture) of the slab occurred also in accordance with the experiment in the transverse direction approximately at the edge of loading plate.

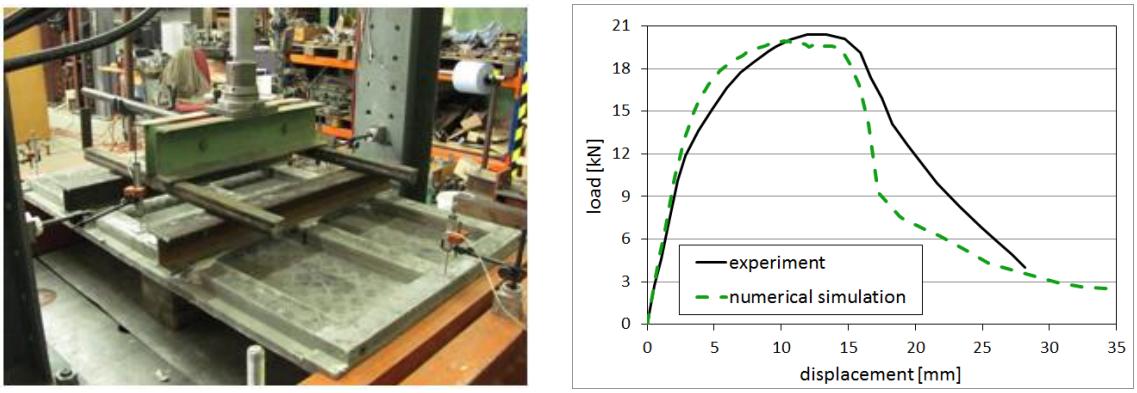

(a) (b)

Figure 13: (a) Four-point bending test of slab, (b) Comparison of experimental and numerical results

3.3 Numerical Simulation of Layered FRC Element

Layered beam designed to sustain bending moment consists of five layers whose fibre volume fraction increases linearly from the upper surface toward the bottom. Fibre volume fractions of all layers are depicted in Figure 14. Total volume fraction is identical with the homogenous beam from the previous chapter, i.e. 1.5 %. Based on the cohesive law for fibre volume fraction 1.5 % derived by inverse

analysis, softening curves for other layers are determined by micromechanical model presented in [26], see Figure 15 (a).

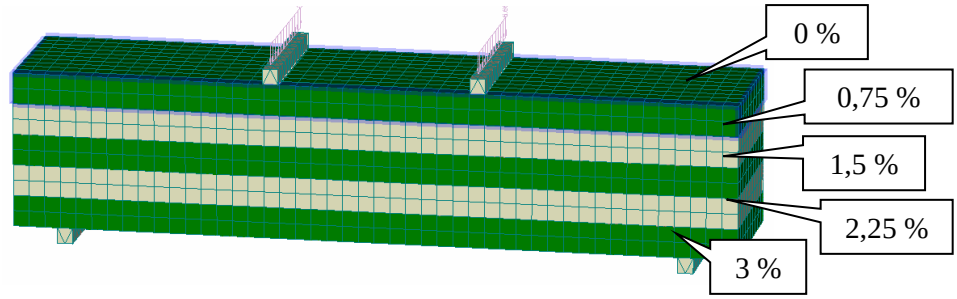

Figure 14: Layered structural element – fibre volume fraction of layers

The spatial variability of mechanical properties was modelled by division of the structural member into macroelements representing different layers of layered member. Each macroelement has specific material model with different fibre volume fraction. Macroelements are connected with each other by an interface with the same properties as the material of macroelements.

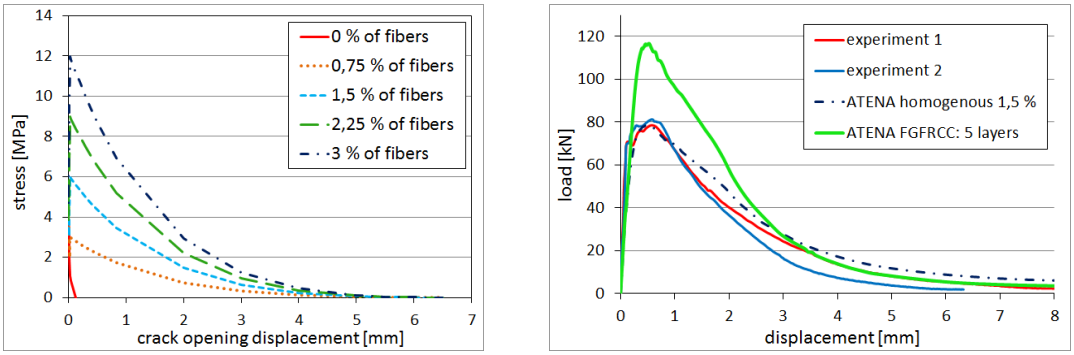

(a) (b)

Figure 15: (a) Softening curves for different fibre volume fraction, (b) Comparison of layered and homogeneous beams

Load-displacement diagram of the layered model is shown in Figure (b) in comparison to the homogenous beam with fibre volume fraction of 1.5 %. The comparison of the curves shows that the layered beam achieves 46% higher load bearing capacity (117 kN compared to 80 kN). Comparison of crack width in the results of numerical analysis is also an important criterion for quality evaluation - at the load of 80 kN maximum crack width in homogenous beam is 0.25 mm while for layered beam it is only 0.012 mm, see Figure 16.

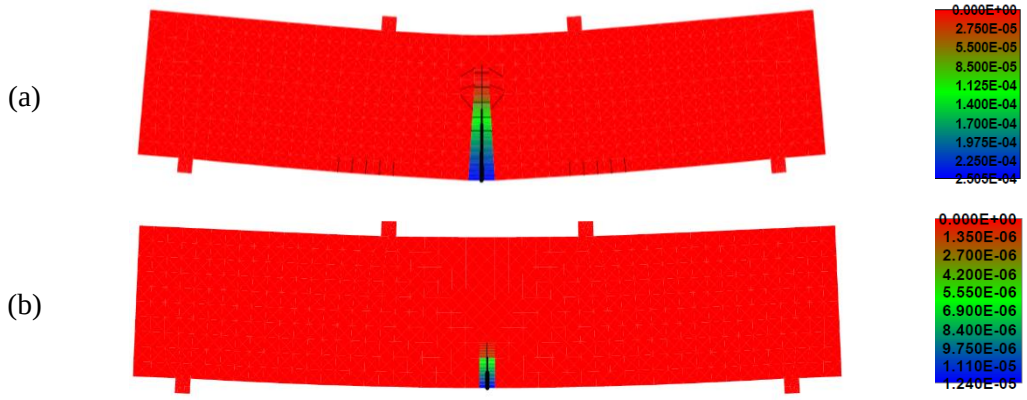

Figure 16: Cracks in beam for load 80 kN – (a) Homogeneous beam, (b) Layered beam

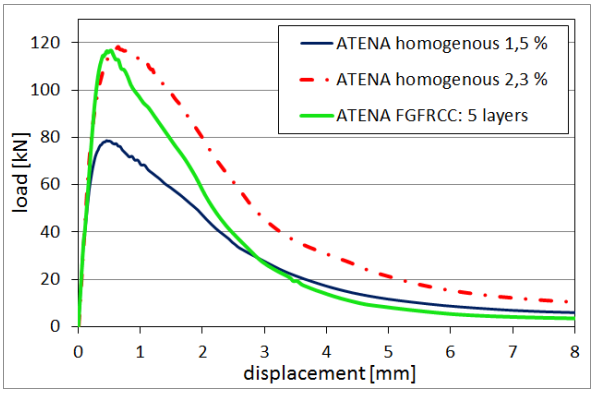

Figure 8: Comparison of homogeneous and layered beams

The results show that the proper arrangement of layers can increase the load bearing capacity by 45 % at the same total quantity of steel fibres. In this specific case, the load bearing capacity of layered element (with a total fibre volume fraction of 1.5 %) is comparable with the load bearing capacity of homogenous element with 2.3 % fibres by volume, see Figure 17. By the nonlinear numerical analysis is shown that it is possible to save 35 % of fibres and still achieve the same load bearing capacity.

The nonlinear finite element modelling can be successfully used for analysis of behaviour and failure of FRC structures. Crack initiation and development, load carrying capacity and post-critical behaviour of the structures, structural parts or experimental specimens can be investigated. Advanced material models for numerical simulation of fibre reinforced concrete are available. Determination of appropriate material parameters for model is of crucial importance. As shown in this chapter, the required values can be efficiently determined using inverse analysis of basic experiments as four-point bending test.

4. Example 2 – Tunnel Tubbing

Two examples of fibre reinforced concrete structural elements are presented in this chapter. The first example is a four point bending beam (see Figure 18).

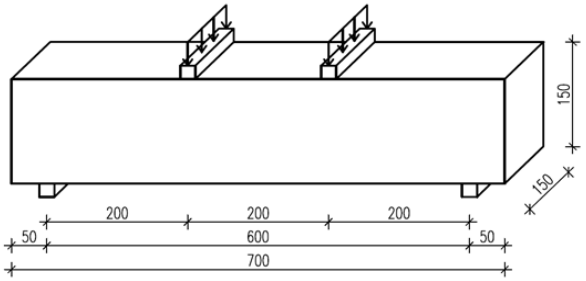

Figure 18: Geometry of the FRC bending beam

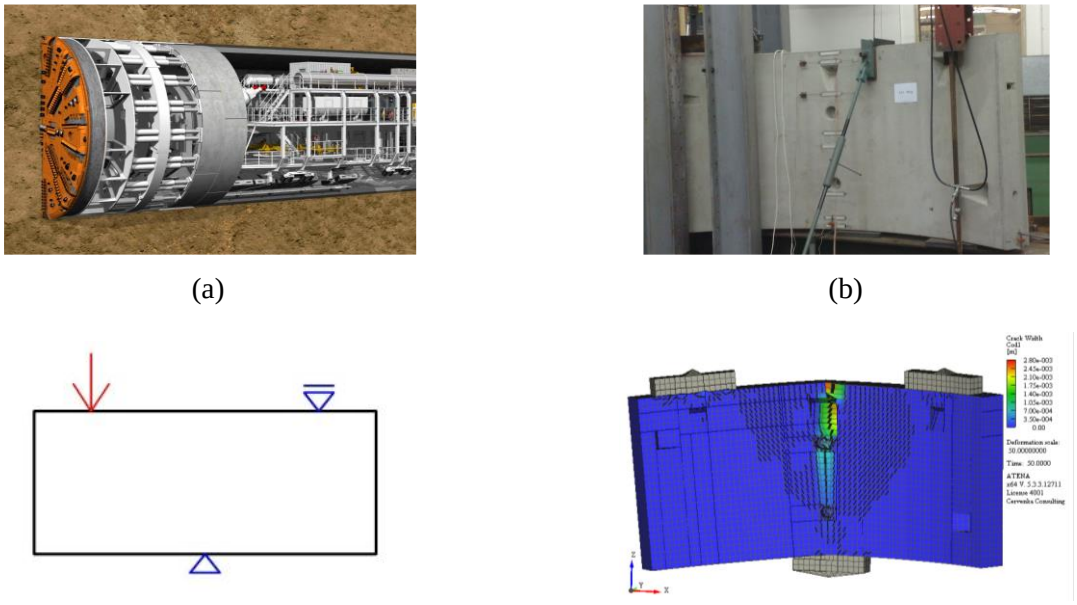

(a) (b)

(c) (d)

Figure 19: Case study example of a tunnel tubing made of fibre reinforced concrete

The mean material parameters were calibrated by inverse analysis described in the previous chapter 2. The second example represents a tunnel lining segment (see Figure 19a) installed by TBM (tunnel boring machine) during tunnel excavation. Full size laboratory tests of both RC and SFRC segments have been performed [24] in the Klokner Institute of CTU in order to check their resistance under various loading conditions. This experimental and analytical program was part of an engineering project in Prague, Czech Republic [30]. Maximum load measured in experiments with SFRC segments was around 500 kN. The numerical model was validated by experimental data for a loading scenario simulating the action of the TBM machine during the installation and assembly of segments (see Figure 19b, c, d).

5. Example 3 - Synthetic and Steel fibres in Prestressed, Precast Long Span Beams

5.1 Test specimens

Four large-scale, prismatic, prestressed, T-shaped beams with 19 m span were produced: two with synthetic fibres and two with steel fibres. The height of the beam was 90 cm, the width of the flange was 50 cm, and the web thickness was 14 cm. Concrete was C50/60-XC1-16, but the first test was made only at 19 days after casting. The homogeneity of the strength was measured by Schmidt hammer.

Six stirrups were placed in the web (height is 45 cm, not reaching the flange), in one meter from the edge of the element to avoid spalling stresses due to the release of the prestressing force, but shear reinforcement was substituted by the fibres (Figure 18). Before the tests 10-40 cm long cracks with 0.05-0.3 mm width were appeared 45-50 cm from the soffit. There were 15-45 cm long cracks with 0.1 mm width between the web and the flange (Figure 20).

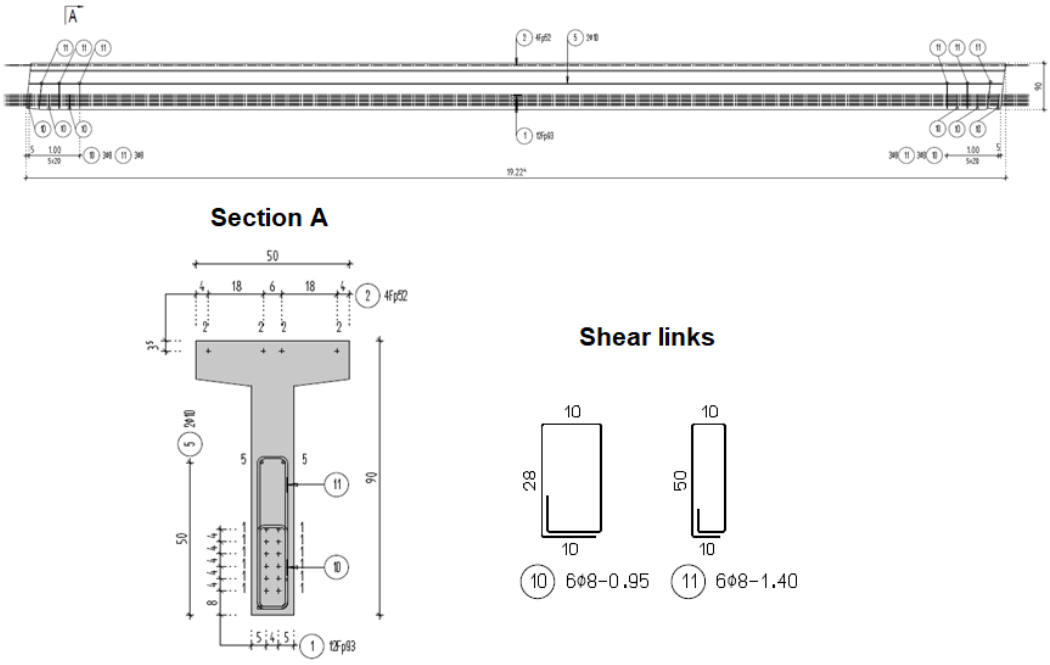

Figure 20: Geometry of the beam

5.2 Laboratory tests

Four point bending test were made to model the built-in behaviour of the beams. The loads were acted in each one-fifth point of the span to be similar to the real load distribution. Force, deflection in the middle of the span, crack patter was recorded in fifteen load-steps. It was decided after reaching the 130% of the design value of the bending resistance, loading will be stopped without a break-off failure to remain the beam-end uncracked for shear tests. A crack with 1.0 mm width was declared failure.

Shear load was affected ~2.5h distance from the beam-end and it was increased until failure. Test and pictures were made by ÉMI-TÜV SÜD Kft, Hungary (Figure 21-22).

Figure 21: Spalling crack in the end of the beam

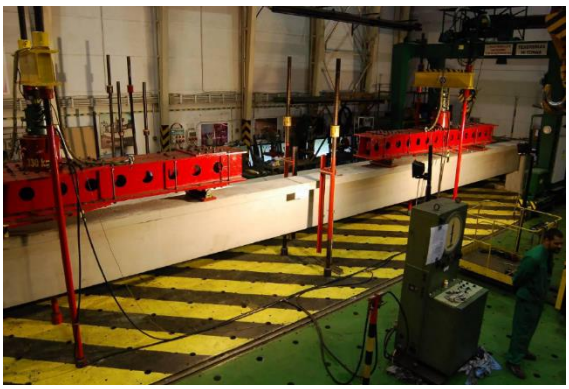

Figure 22: Bending (left) and shear (right) tests

5.3 Results for Bending Beams

Beams made of steel and synthetic fibre reinforced concrete showed similar load bearing behaviour during bending tests. Cracks appeared regularly and frequently between the two outside press, the beam end remained uncracked. As the load was increased, cracks started to open and reached the flange. Cracks with 1.0 mm width were appeared at 120% of the design value of the bending resistance, but they closed due to the high prestressing force after deloading.

In case of synthetic fibres the crack propagation process started earlier, at lower loading level, was faster and cracks were closer to each other. In the seventh load step inclined (~45°) cracks appeared at the outside loads. In case of steel fibres the same was observed only in tenth. After two loading level their width was the same as pure bending cracks'. Other new cracks' inclination was lower. In the last loading level they reached 1.0 mm width. Failure was observed at the shear-bending zone with obvious prognostic in both cases.

Figure 23: Failure of the element

5.4 Results for Shear Beams

In the shear tests first cracks appeared at 115% of the design value of the shear resistance. Failure with 1.0 mm width was observed at 200%, the break off was at 230%. All the cracks went from the support to the load, the firsts' inclination was 35-45°, and the last was 18°. Failure was ductile in cases of both steel and synthetic fibres.

Figure 24: Bending (left) and shear (right) tests

5.5 Material Model of the Concrete and FRC

The effect of the fibre in the concrete was investigated in previous grandstand concrete elements at the new stadium in Debrecen, Hungary. Four point beam test were made on 150 mm x 150 mm and 550 mm long beams, according to RILEM TC162. After the results, inverse analysis was made and the

correct added fracture energy (G_{Ff}) was measured by fibre dosage. The crack-width diagram was defined until 4 mm crack opening as a limit from an engineering point of view.

The finite element model used the following material parameters for fibre reinforced concrete:

Elastic modulus:	37GPa
Tensile strength:	4.1 MPa
Compressive strength:	58MPa
Poisson ratio:	0.2
Residual flexural strength:	0.97 MPa
Fracture energy of the concrete:	0.103 kN/m

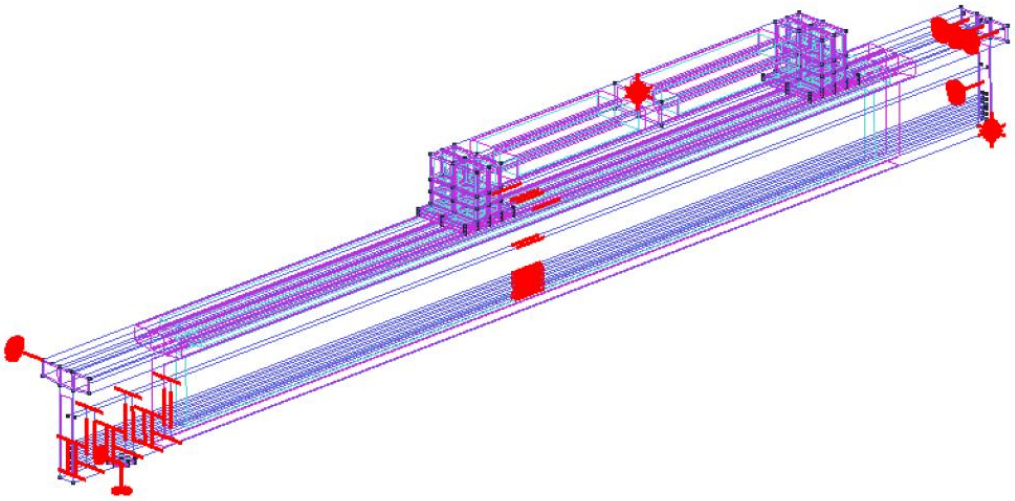

Figure 25: Simplified model in Atena finite element program

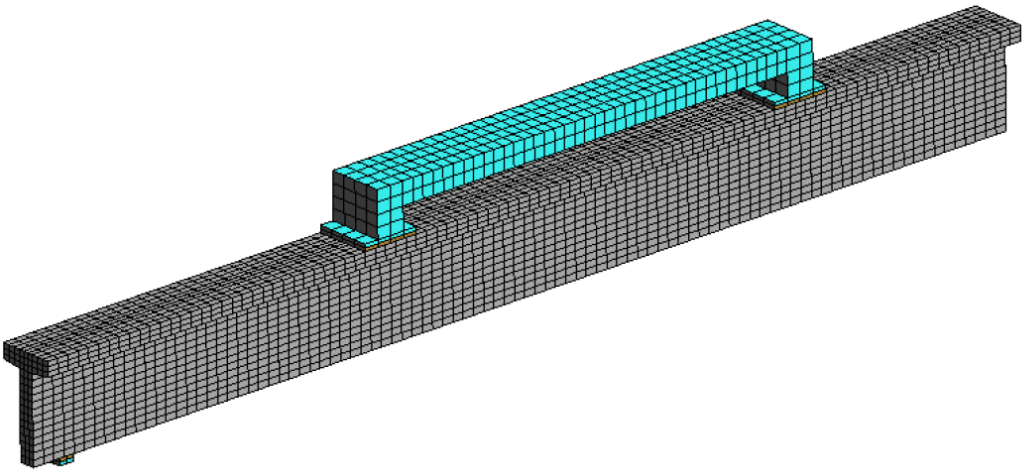

Figure 26: Structural mesh in Atena finite element program

5.6 Numerical and Test Results

The numerical calculation shows good correlation with the test result. The fibre reinforced concrete beam has the maximum bending capacity 52% higher than the plain concrete one.

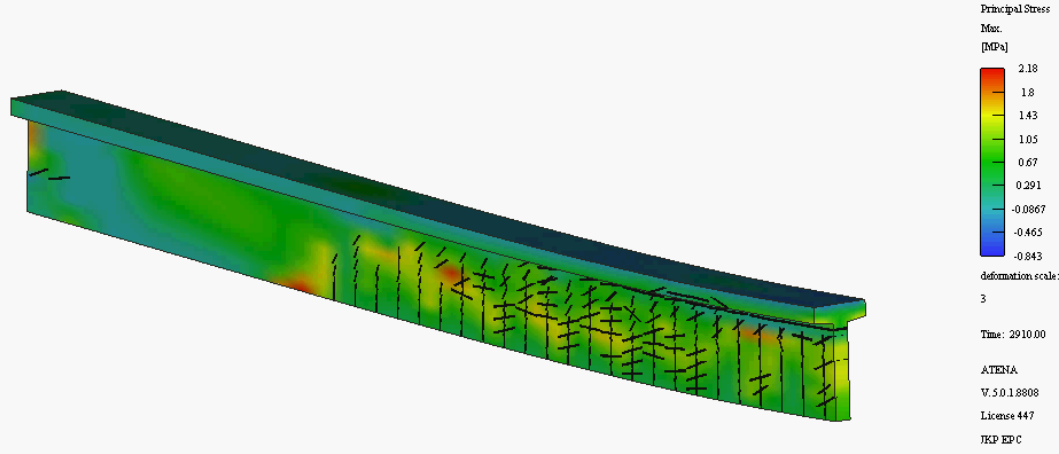

Figure 27: Principal stresses and cracks in Atena finite element program

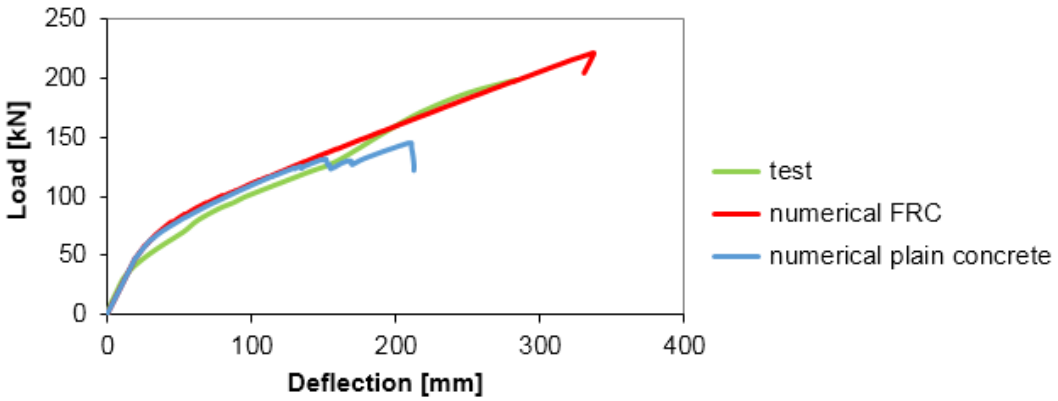

Figure 28: Test and numerical load-deflection results

5.7 Conclusion

The structural behaviour was clear, but advanced statistical analysis cannot be performed due to the limited number of beams. The existence of horizontal spalling cracks on the beam ends was predicted by the verified finite element analysis. Calculation shows higher dosage of fibres or extra reinforcement is needed to avoid spalling failure, although these cracks do not influence the load bearing capacity of the beam.

There was no difference between steel and polymer fibre reinforced concrete beams in load bearing capacity. In the four-point bending test failure occurred in the bended-sheared area by inclined cracks, although the crack-width in the pure-bended zone was also remarkable. Inclined shear crack with 1.0 mm width was achieved at the same load level in the two cases. Breaking shear load was 25% higher, showing tough behaviour. Breaking was ductile with obvious prognostic. The cracked surface was examined, the fibres mostly pulled out instead of tearing. Finite element analysis shows significantly higher (52%) load bearing capacity of the fibre reinforced beam compared to plain concrete one.

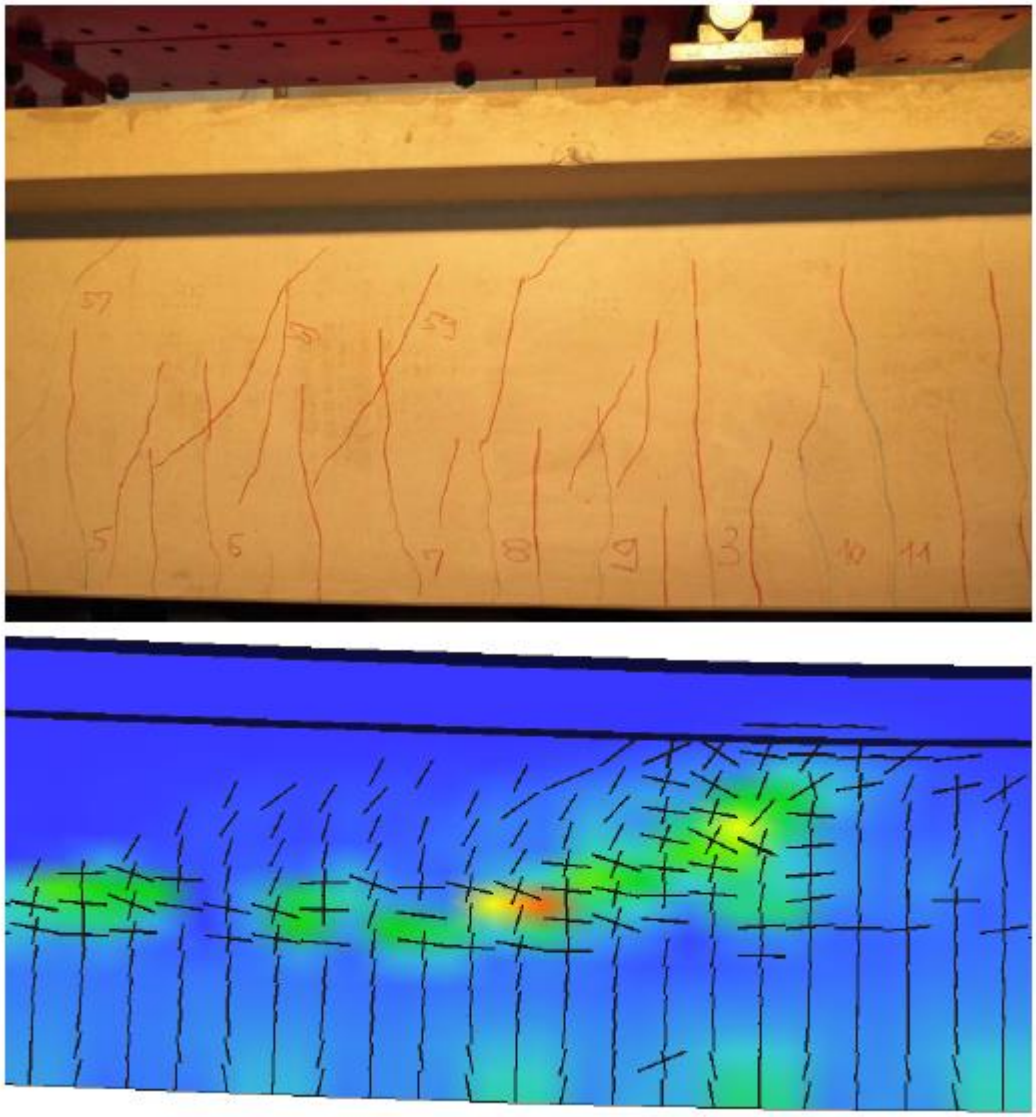

Figure 29: Test and numerical crack propagation

6. Example 4 - Prestressed Reinforced Concrete Grandstand Reinforced with Synthetic Macro Fibres

One element of the precast reinforced concrete stadium is the grandstand. Current case study is about the design and laboratory testing of a prestressed reinforced concrete grandstand reinforced with synthetic macro fibre. Due to the complex geometry of the grandstand manufacturing and positioning of the shear stirrups is costly, therefore in order to lessen the costs and to speed up the manufacturing stirrups will be replaced by synthetic macro fibre. Choosing the synthetic fibre-reinforcement was a reasonable decision to avoid corrosion, as the grandstand is continuously exposed to weather conditions.

6.1 Laboratory tests

Based on a comparative study the fibre with the highest R_{e3} value was chosen. R_{e3} number could be determined according to the Japanese standard JSCE SF-4. During the comparison beams were manufactured with the same dosage and the same concrete but with different fibre types, which were then tested at the same time. The chosen fibre was a 48 mm long, surface embossed polypropylene fibre (BarChip 48). Further beam tests were done from the chosen fibre with the fibre dosage being 2.5, 5 and 10 kg. Material properties with the fibre dosage of 3, 3.5, 4 and 4.5 were defined with linear interpolation. Concrete strength class was C40/50.

The grandstand was simulated by considering the following load cases: 1) loaded in the whole standing area; 2) loaded only in the lower standing level; 3) loaded in the upper standing level; 4) loading and unloading; and 5) dynamic loading. Load combinations and safety factors were used according to the Eurocode.

Material parameters of the fibre reinforcement were defined by inverse analysis using the results from three point notched bending beam test according to the recommendations of MC2010. The finite element model was loaded by displacement control exactly how the real tests were carried out.

6.2 Material Model of the Concrete and FRC

Material parameters – concrete (mean values, concrete strength class: C30/37)

Elastic modulus:	32 GPa
Poisson coefficient:	0.2
Tensile strength:	2.9 MPa
Compressive strength:	38 MPa
Fracture energy:	0.073 N/mm
Aggregate interlock activated, d_{max}:	20mm
Plastic strain:	0.00119

Material parameters – FRC

Added fracture energy, G_{Ff}:	2.7 N/mm

Material parameters – tendon

Elastic modulus:	195 GPa
Characteristic yield strength:	1860 MPa
Yield strength:	2046 MPa
Initial prestressing:	865 MPa

6.3 Numerical and Test Results

6 real-size elements were made, from which 4 were macro fibre-reinforced and 2 were made without fibre reinforcement, but with traditional shear stirrup reinforcement. Bending and shear tests were made under laboratory conditions. Elements were loaded on both stairs continuously, loads, deflection (vertical displacement: in front of and in the back of the element in the middle and in both ends; horizontal displacement: only in the middle of the grandstand) and crack patterns were recorded. Results show all of the elements met the requirements specified (at SLS: maximum deflection of l/250, maximum crack width of 0.3 mm) and carried the load in the same way.

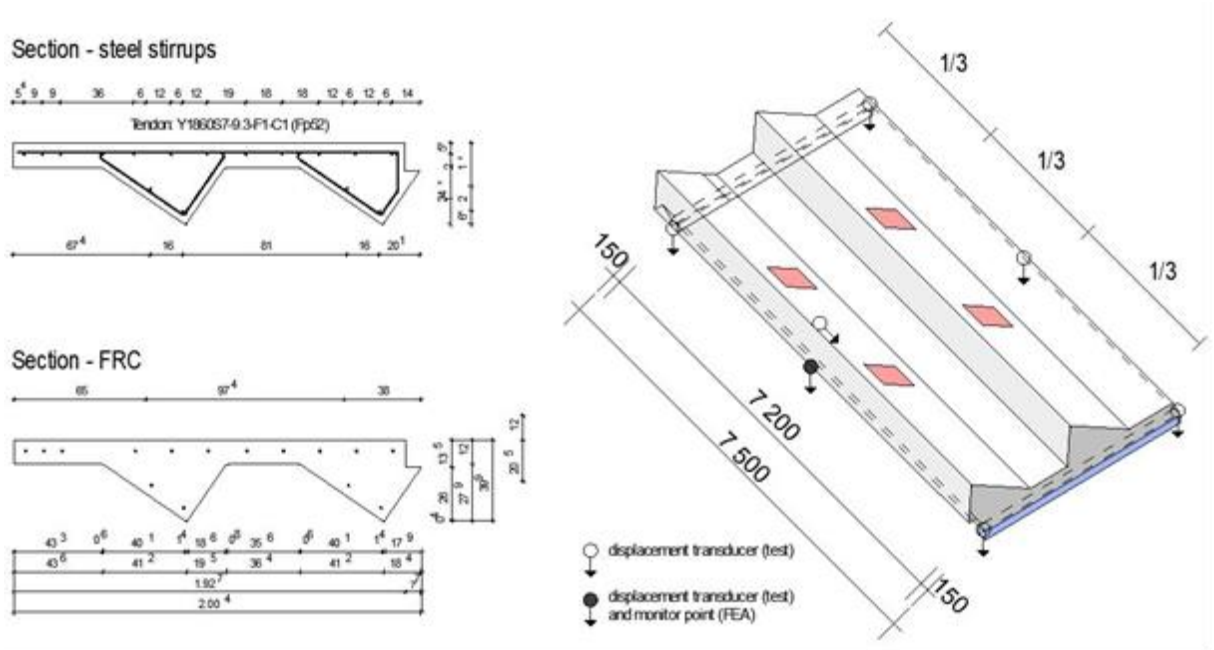

Figure 30: cross section (left) laboratory setup (right)

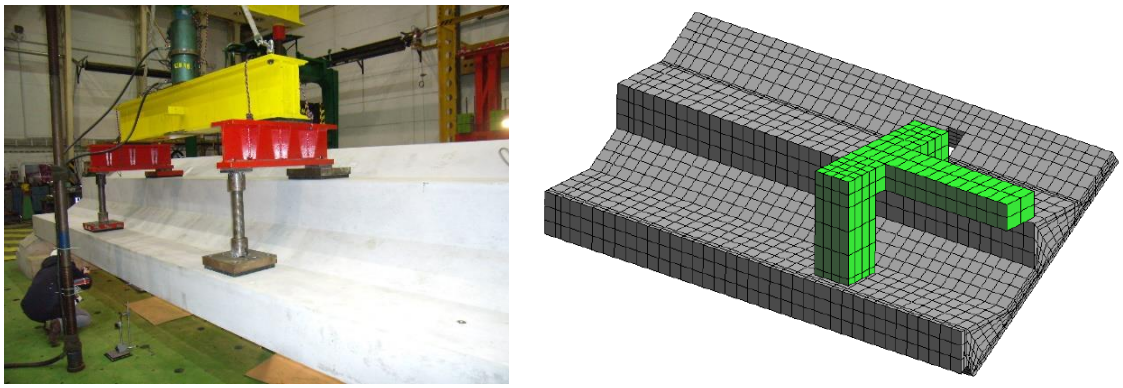

Figure 31: Laboratory test (left) numerical model (right)

Numerical results fit the real test results well, thus further finite-element calculations were made with different dosages. The optimal dosage defined was therefore 3 kg/m^3.

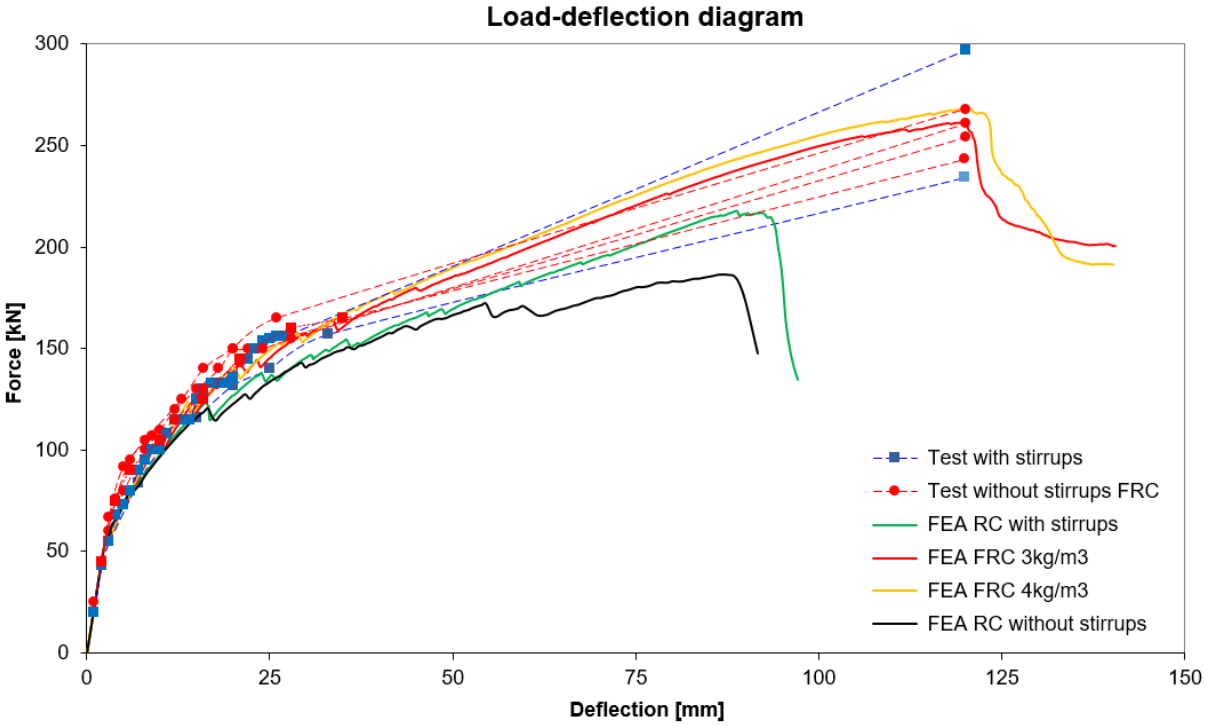

Figure 32: Load and deflection diagram of test and FEA

The maximum crack widths on the upper and lower surface of the grandstand were measured during the test at different loads: 95 kN, 115 kN, 125 kN, 145 kN, 165 kN, 190 kN (or 200 kN). The maximum crack width on the lower surface was obtained also in ATENA by selecting the elements near the surface at different deflections. At the laboratory test the maximum crack width was near the failure point, in the middle of the specimen, while at the ATENA model the maximum crack width was near the leg of the loading frame. The comparison between the results of the crack width on the lower surface of the laboratory tests and the numerical results can be seen on Figure 33.

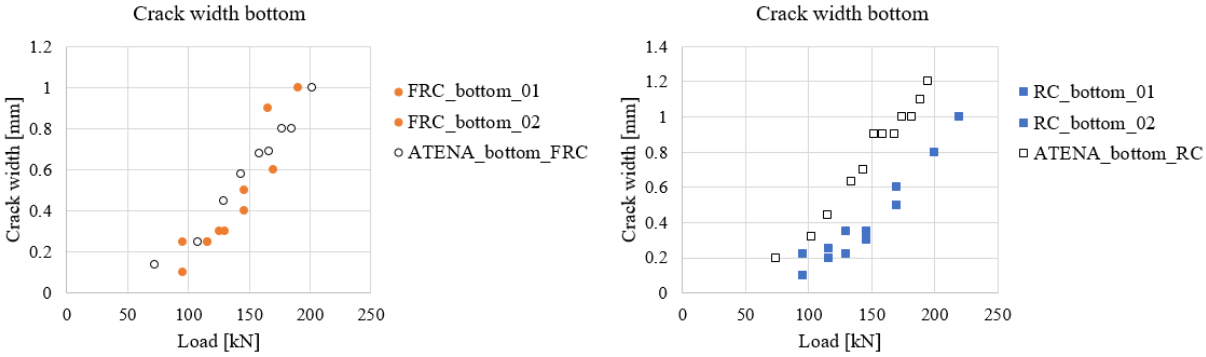

Figure 33: Crack width on the lower surface of the grandstand element

7. Example 5 – Industrial Floor

The use of fibre reinforcement has become a popular alternative to traditional steel mesh in industrial floors for the control of early age shrinkage. However, there are no generally accepted standards for the design of the jointless floors, only guidelines. One of the most well-known guidelines for industrial floors is the British guideline: TR 34 – Concrete Industrial Ground Floors. In the 4th edition the calculation method of early age shrinkage was totally omitted, and the document limits itself to simply stating that cracks could be avoided if the concrete mix design, curing time and dilatation distances are appropriate and well designed. The results of different age tests were implemented into an advanced Finite Element Analysis, with a time-dependent material model which enabled the simulation of the effect of the fibres on the crack propagation during the hardening of the concrete in an industrial floor. The connection to the subbase was modelled with different interface elements to model the slip effect. Results show clearly the difference between plain, steel and synthetic fibre reinforced concrete materials.

7.1 Material model

The material model of concrete consists of a combined fracture-plastic failure surface. Tension is handled herein by a fracture model, based on the classical orthotropic smeared crack formulation and the crack band approach. It employs the Rankine cube failure criterion with a fixed crack model (rotated crack model was not suitable for this calculation). Aggregate interlock was taken into account by reducing the shear modulus with growing strain along the crack plane. The effect of the fibres was calculated with the modified fracture energy method [16]. The added fracture energy was calculated by inverse analysis.

All of these parameters of the plain and fibre reinforced concrete were implemented into a time-dependent material, where the parameters were changed in every step during the calculation. The parameters of the time-dependent material model could be seen in Table 1. Shrinkage strain was calculated according to Japanese standards until day 232. Relative humidity was set to 60% and the water content was 160 kg/m^3.

Table 1: Time dependent material parameters

Time	Step	Strain ε_{cs} x 10^5	Elastic modulus E [GPa]	Tension strength f_t [MPa]	Compressive strength f_c [MPa]	Fracture energy G_f [N/m]
9 h	20	1.91	4.5	0.0365	1.14	0.217
14 h	258	2.59	7.5	0.38	2.28	12.1
1 d	563	3.44	16.5	1.027	9.5	27.6
7 d	2612	9.30	29.1	2.375	28.5	59.6
28 d	5319	17.01	30	2.70	38	72.5
232 d	10020	30.39	30	2.70	38	72.5

Soil was modelled with a linear material model with an elastic modulus E=30GPa. Between the soil and the concrete there is a contact element (GAP) with three different types of strengths: 1) fix contact, F-

series; 2) cohesion of 0.3 MPa, M-series; 3) cohesion of 0.06 MPa, L-series. The different contact elements are modelling the different subbases and layers under the concrete slab.

7.2 Numerical model and intervals

The industrial floor was modelled with ATENA Science FE software in 2D with plane strain idealisation. The dimensions and supports can be seen in Figure 32. The mesh size was 6.66 cm (1/3 of the slab thickness) x 10 cm. Three main intervals were used: int-1) for calculating the own weight of the floor; int-2) for calculating until the end of the curing time; and int-3) for calculating until day 232.

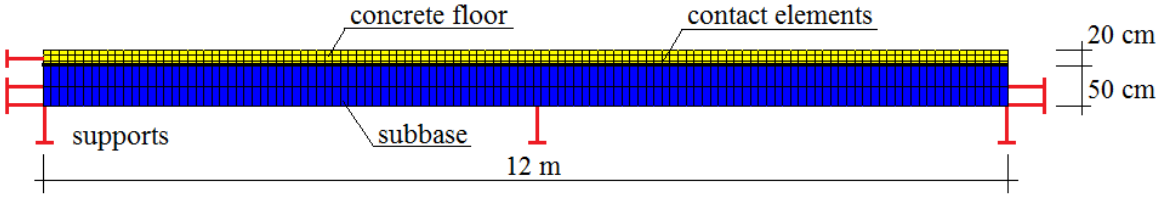

Figure 34: Numerical model of the industrial floor

7.3 Results

The relationship between the dosage and the maximum crack at different contact element types can be seen in Figure 35. The effect of fibre reinforcement shows significant differences at each type of contacts. The biggest effect can be reached at the soft connection, which is modelling the traditional industrial floor layers, e.g. 2 layers of PE folia. This effect goes up to even 30%, depending on the dosage. The dosage and maximum crack width shows direct proportionality. At the contact with medium stiffness the increase of dosage has limited advantages, thus low dosage seems to be the optimal solution. At fix contact there is no significant effect of the use of fibre. The crack propagation at plain concrete and FRC can be seen in Figure 36. It is also notable that the displacement of the fibre reinforced concrete slab is bigger than the plain concrete at the free edge.

The increase of the crack width as a function of time could be seen in Figure 37. This curve has the same characteristic as the time-shrinkage diagram. Obviously, there is no tearing at the connection in case of fix contact. The separation is a continuous process in case of soft connection, and results in a smooth curve, while, in case of medium connection the curve has a break point.

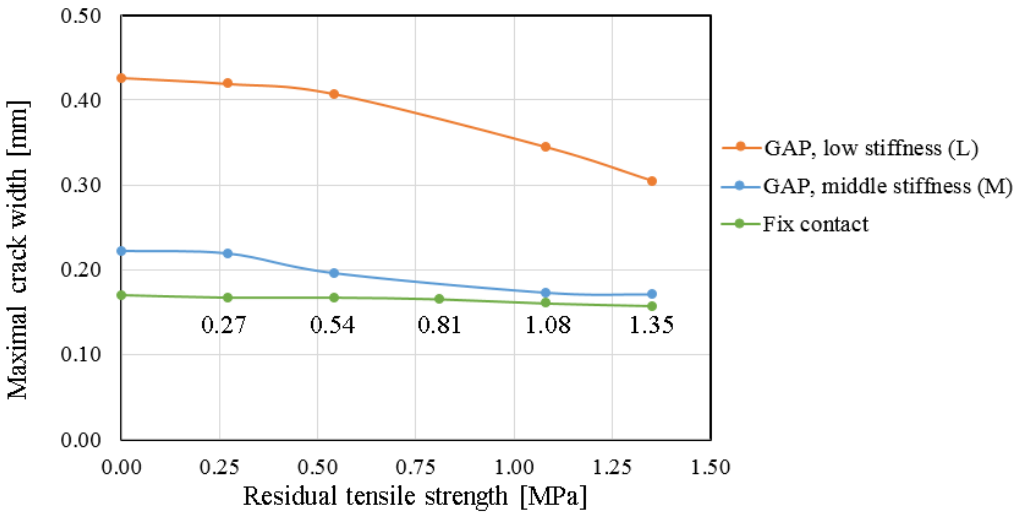

Figure 35: Residual tensile strength and maximum crack width relationship

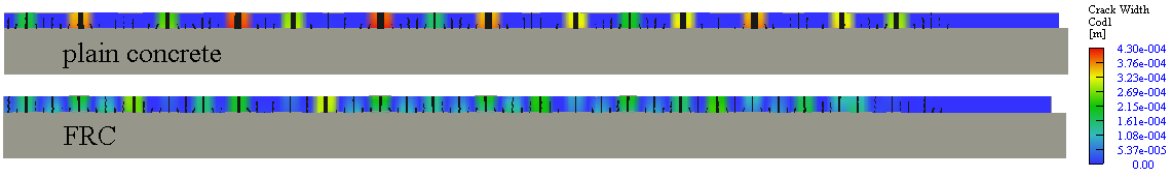

Figure 36: Crack propagation at plain concrete and FRC

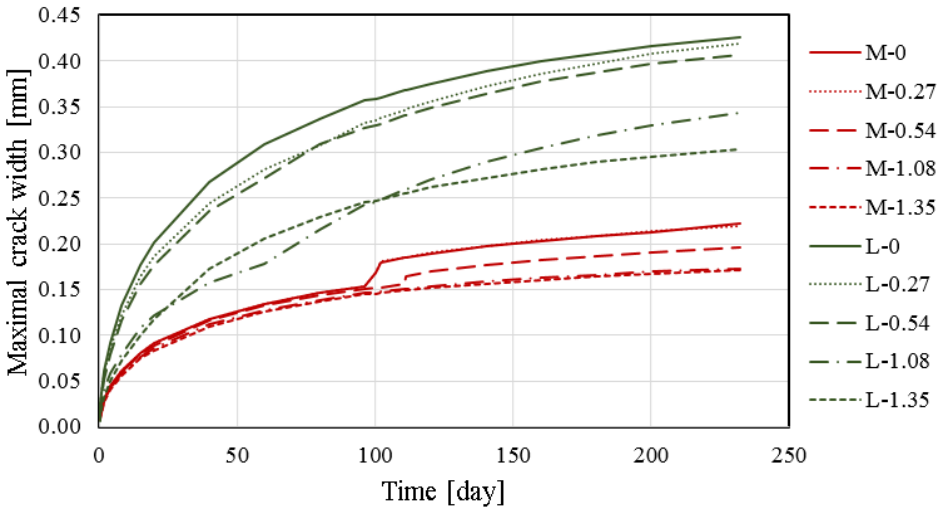

Figure 37: Increase of crack width as a function of time

7.4 Conclusion

Effects of the fibres for preventing or reducing the early age cracking are well-know, although none of the standards or guidelines takes into account this advantage. After cracks appear the post-crack performance of the fibres are different: micro fibres have only limited residual tension strength, while macro fibres have significant value. The capacity of the fibres during hardening is also different, in this case it depends on the material: steel fibre has a limited capacity until the first day, while synthetic macro could work from the beginning of the life of the concrete. During the curing time of the concrete of an industrial floor the concrete could crack. In this case micro fibres cannot prevent the crack opening, only macro fibres. The crack propagation and maximum crack width mostly depends on the fibre type, dosage and the connection between the floor and the subbase. The results of the beam tests were implemented into a time-dependent material model and FEA was done on a simple industrial floor structure. Results of the numerical research showed that also macro fibres have effect on the early age crack propagation, although these fibres mostly start working after the cracks appear. The maximum crack width and crack propagation were researched as a function of time. Research also showed that the effect of the fibre mostly depends on its dosage and the stiffness and strength of the contact between the industrial floor and subbase.

8. Example 6 – Tramline

Today the construction of modern concrete slab track plays a prominent role in the construction industry. Besides keeping in mind having an economic solution, more emphasis is placed on its durability and its resistance to environmental factors such as moisture, de-icing salts etc. The economic solution can be achieved primarily by decreasing the thickness of the slab and shortening the construction time. Durability can be significantly increased by designing for fatigue and by using materials that are resistant to these environmental factors. Because of this macro synthetic fibres are being used more often for the reinforcement of the concrete for both cast in place or precast structures.

Corrosion resistance is the greatest benefit of macro synthetic fibre where durability can be assured but also synthetic fibres behave better with dynamic loads than steel fibres, therefore their use for tramline or railway track slab is very favourable. Added to this are the economic advantages such as a reduction in labour that would traditionally set and tie the steel reinforcement into place.

The first macro synthetic fibre reinforced track slab was constructed in Japan in 2002: Elasto Ballast track railway. The goal of using macro synthetic fibre was, beside from the reduction of the vibration and noise, to increase the speed of the construction process. The track slab was made using a traditional slab structure with pre-stressed concrete sleepers on it supporting the rails (Figure 38). The reinforcement was a hybrid of traditional steel bar reinforcement together with macro synthetic.

Figure 38: Elasto Ballast track railway

The first synthetic fibre reinforced track slab in Europe was the Docklands Light Railway near London in 2004. The slab was reinforced with 6 kg/m^3 macro synthetic fibre reinforcement (BarChip48 high quality macro syntethic fibre) which made the construction process considerably faster.

The first only macro synthetic fibre concrete cast in place tramline in Europe was built in Szeged, Hungary. Macro synthetic fibre was considered over steel reinforcement as at a certain point in the track it was not possible to use any steel reinforcement due to the operation of a special switch that collected stray current and so this part of the track was reinforced with macro synthetic fibre**s**Because of the positive experiences and cost saving in this part of the track the contractor changed to this solution for the entire track and thus replaced all the steel reinforcement with macro synthetic fibres.

Beside the cast in place solution the use of precast concrete tramline elements started to spread, mainly because of the same benefits of shortening construction time. These elements also needed to be designed for temporary situations, such as demoulding, lifting, transporting and placing on site. The first and only macro synthetic fibre reinforced precast concrete track to date is the PreCast Advanced Truck (PCAT) system. This precast element is highly optimised both by the dosage of the fibre and its geometrical shape.

8.1 Cast in place tramlines

One of the most common structures for tramlines is the cast in place track slab. There are several proprietary track slab configurations commonly using either the poured in place form worked track slab or the track slab extruding machine. In the first case after installing the formwork the slab is filled with macro synthetic fibre reinforced concrete, and the joints are installed after each section of the track slab is poured. Each pour is then mostly connected with steel dowels. In the second case the machine continuously pours the macro synthetic fibre reinforced concrete between the moving formwork. In this case the joints are made by saw cutting the slab, which reduces the likelihood of any crack formation.

8.2 Szeged tramline

In 2010 and 2011, during the extension and reconstruction process of the A and C sections of tramline Nr. 1 in Szeged (Figure 39) in an areas of the so-called loops which was a major tram intersection, it was necessary to have concrete track slabs that contained no steel reinforcement. Therefore, it was an idea to use macro synthetic fibre-reinforced concrete in these sections. At that time, only synthetic microfibers had been used for concrete reinforcement in Hungary, the effects of which are mostly seen in the case of fresh concrete: through reducing the rate of plastic shrinkage cracking. However, in hardened concrete only macro synthetic fibres have any structural impact. While exploring foreign technologies, it was found a suitable building material for this purpose a Japanese-developed macro synthetic fibre. During the design process it turned out that traditional reinforcement could entirely be replaced by the use of this macro synthetic fibre in this application. After a technical and financial analysis it also became clear to the general contractor that the desired structure could be built more economically and faster, furthermore: not only could it be applied in the critical sections where no steel reinforcement was allowed, but also it could be used in the other sections of the tram tracks. Based on the above, a unanimous consensus was reached by the Client, the General Contractor and the Designer to try out the new technology. The new technology was designed for and initially tested on non-critical track areas (RAFS-CDM) such as at road junctions, turn-outs, current tracks, bus bays and vibration damping tram tracks.

Figure 39: Tram line in Szeged, Hungary

During the design process the dynamic loads of trams and buses were taken into account, then the load-bearing capacity, serviceability and fatigue limits were checked in accordance with Eurocode. Finite element analysis was made on the basis of the recorded material model recommended by RILEM TC 162-TDF. According to the calculations the tramway met the standard loads and load combinations.

8.3 Tramlines around the world

The Szeged tramway project was a huge success. After the system proved to be fully functional several other tram tracks were constructed using very similar solutions and using macro synthetic fibres. These tram tracks were constructed in St. Petersburg, Russia, and in Tallinn, Estonia. In Hungary the success also continued and led to the partial reconstruction of Budapest tramlines Nr. 18 and Nr. 1, as well as the complete track reconstruction of the Nr. 3 tramline using this solution.

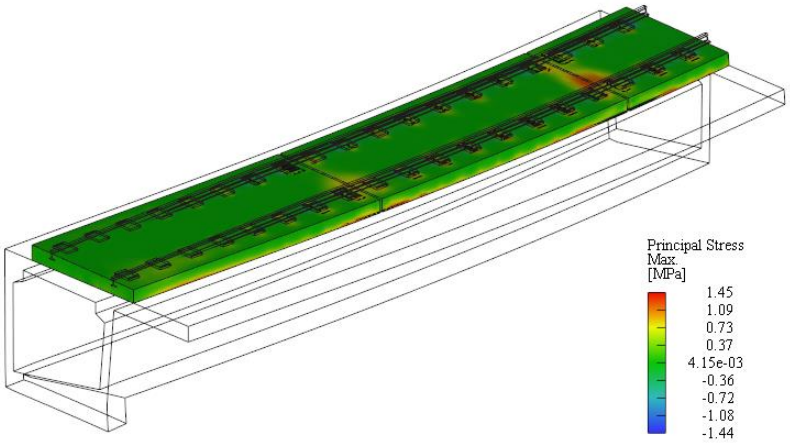

Figure 40: Tramline on a viaduct calculation with ATENA

8.4 Precast concrete tramlines

Another important trend in tramline structures is the precast concrete track slabs. These elements are made in precast concrete factories and transported to site. These elements will be subjected to other loads beside above their final load cases such as early age demoulding, rotation, lifting, stacking, transporting and installation on site. Usually these elements are made from concrete with higher strengths i.e. from C40/50 than the cast in place slabs i.e. from C25/30. Generally the precast elements have a higher dosage of macro synthetic fibre to the track slabs that are cast in place.

8.5 The PCAT system

PreCast Advanced Track's (PCAT) unique 100 per cent macro synthetic fibre reinforced precast concrete slab structure is set to revolutionise the construction and repair of the world's railways. PCAT's innovative lightweight slab structure represents a world first for precast track slabs as it is manufactured entirely from macro synthetic fibre reinforced concrete without steel reinforcement being required. This ensures that if the concrete cracks there is no steel to corrode providing a long life structure, as fibres continue right to the edge of the structure and so enhances durability and resistance to accidental damage. It also reduces maintenance, material costs and the fibre reinforcement is safer to handle than steel during manufacture. The PCAT slab design is based on a channel beam upper profile which provides a high modulus slab structure which maximising the slab's strength and minimises the stiffness needed for the track foundation. This allows PCAT tracks to be constructed quicker than conventional track.

The slabs connect to each other with a dry male-female joint for initial alignment and then with curved bolt connections. This is designed to permit the rapid laying and joining process to form the monolithic structure. Curved steel connectors between adjacent units are easily inserted and tensioned from the slab surface as erection proceeds. This allows rapid installation to take place from the newly laid track even in tunnels with restricted space. Uniquely, if needed, PCAT slabs can be simply decoupled, levels adjusted or slabs removed and replaced without affecting the rest of the track structure.

Two types of slabs were developed to serve all potential installation requirements. One is aforementioned standard slab (off-street slab) with the side beams which is highly optimised and can easily installed. The other one is a more robust structure but with a straight upper surface and with hidden rails (on-street slab). This type of the slab can be used in streets and thanks to the sunken rails the traffic can easily cross the slab. The maximum length of both types is 5000 mm, the minimum thickness of the off-street slab is 150 mm and the thickness under the rails in case of on-street slab is 200 mm. The slabs were designed for 120 year lifetime.

8.6 Finite element model of the structure

The numerical modelling of the PCAT slabs was done with ATENA finite element software. The finite element models of the structures can be seen in Figure 41.

To ensure that the design model reflected the real structure's behaviour, all the details were modelled including the connection ducts, the injection holes, the rail sleepers and the rails with their exact geometry. A one and a one half slab was modelled to be able to investigate the behaviour of the joints. For the connecting surface an interface material was determined, which could only support compression stresses. During the loading process it was found that the slabs could open along the connection surface and the ducts bear the tension stresses. Under the slabs a bedding layer and a HBM (Hydraulically Bound Mixture) layer was modelled. For the subgrade non-linear springs were used. To investigate the effect of the soil parameters all the models were checked for a higher (350 MPa) and a lower (175 MPa) stiffness HBM layer.

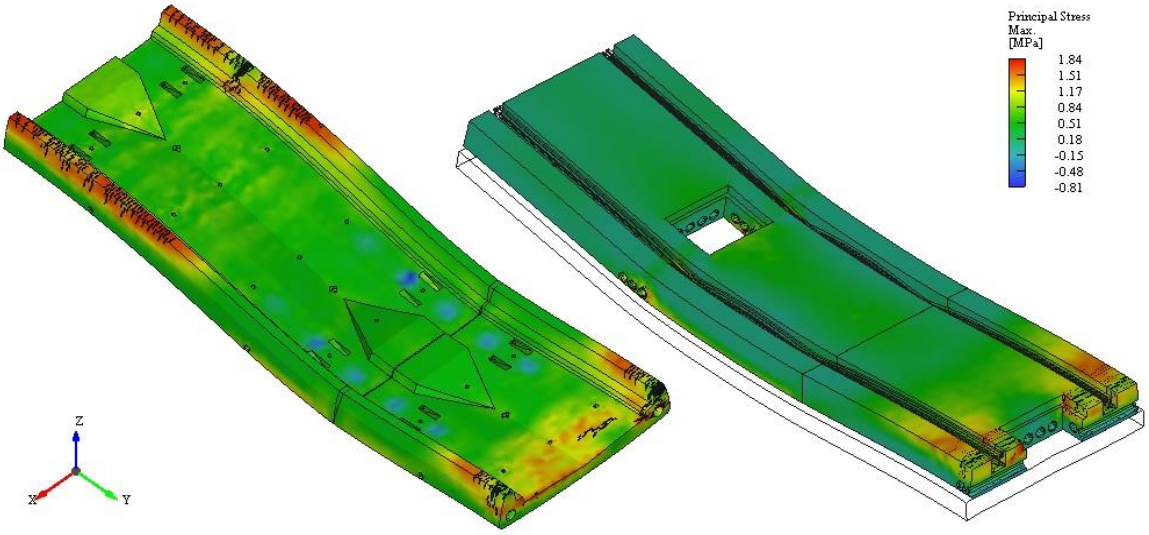

Figure 41: Principal stresses and cracks in deformed ATENA model

In the model various material model configurations were used for the different structural elements. For the concrete slab the previously presented concrete material was used. For modelling the subbase and the subgrade linear elastic materials were used with different elastic moduli. The same material model was used for the sleepers as well. For the steel elements, such as the rails and connection cables a Von Misses material model was used which could handle the yield of the steel elements. Two different interface elements were used, one to model the friction between the concrete slab and the steel duct, and one to model the transfer of the compression forces between the two slabs. The parameters were determined in both cases to be as close to the real behaviour as possible.

To check all the possible effects on the slabs, different loading scenarios were carried out in the finite element software as its lifecycle the track slab will be subjected to various conditions. Because the slab is pre-casted the first loading will come from demoulding of the element. In this case a time dependent material model was used, which means the material parameters changed during the analysis following the hardening of the concrete. With this analysis the optimum demoulding time can be estimated as well. To the demoulding load a lifting and tearing force was added to the early age concrete slab. After this, but also in early ages, a rotation effect occurs: the demoulding was made upside down, but the racking of the precast slabs were in the other direction. In this two load case the lifting and rotating of the elements were also checked. The next situation was the storing load case. In this case the weight of three elements was added to the slab, simulating the effect of the stacking. The highlighted design target was to check the ultimate and serviceability limit states under the train's load and thus the geometry of the trains were added. To examine the worst loading case, and to model the passage of the train, seven different loading scenarios were carried out in different positions. In the Ultimate Limit State (ULS) the principal stresses were checked and in the Serviceability Limit State (SLS) the crack widths and the vertical displacements were checked. During the calculation the unequal rail loading was also taken into consideration. To be able to calculate the effect of the cyclic loading fatigue analysis was done also for all the loading positions. The number of the cycles was calculated back from the estimated lifetime of the structure and the average daily traffic. The finite element software calculated two additional fatigue strains for the maximum fracturing strain, one handled the tensile strength reduction during the cyclic load (according to the Wöhler curve), and the other takes into consideration the crack opening effect during the cyclic load.

The structure complied with all the design requirements both in ULS and in SLS. In ULS the target was that the structure resists the loads with the appropriate safety factors and with design material parameter values without the failure of the structure. In SLS the aim was that the crack widths should be less than the value according to Eurocode 2 (0.2 mm). Both design cases met the requirements in every loading position and design situation.

The slabs deformation was realistic and it followed the expectation under the different loads. The connection between the two slabs worked well. It also can be seen that the structure is highly optimized. In ULS several cracks appeared in the surface of the structure, but without failure, and in SLS almost no visible cracks appeared in the structure.

Figure 42: The test line of the PCAT system

8.7 Real scale test

The PCAT slab was installed within their test pit to measure the actual deflection of the slab along the structure using an applied load at various locations. The position of the load was replicated the arrangement used in the FEM simulation. The PCAT off-street slab was designed for 12 tonne axle loads. For the testing it was proposed, after the first suite of loading at 8 tonne that the load be increased in 4 tonne increments up to 24 tonne, subject to slab performance during the test.

The loading of the slab was carried out using the Rail Trackform Stiffness Tester (RTST) (Figure 43) which was been developed by AECOM to replicate the loading requirements of high-speed or heavy-haul lines through the use of an increased range of pulse-loading conditions. The RTST apparatus is mounted on a transport frame that can be moved along on rubber-caterpillar tracks whilst off track and then switched to rail wheels. On ballasted track geophones measure the deflection response of the ballast, sub-ballast, formation and subgrade enabling assessment of layer stiffness. During testing of the PCAT slab an array of 9 geophones were positioned above the concrete slab surface to record the deflection in microns.

To ensure the numerical model's property, a finite element analysis was calculated for the RTST test. The model contained the whole test setup including: the concrete pit, the compacted soil, and the two slabs with the previously mentioned detail. The effect of the RTST was added to the slab with using a steel plate which corresponds to the loading beam's foot. The measured value in the finite element model was the vertical deflection. It was measured at 9 different points replicating where the geophones were

positioned for the actual test. The position of the loading plate in the finite element model followed the RTST machines position in the test.

Figure 43: The RTST testing (AECOM PCAT Test report)

The results in every loading case were close to each other. The finite element analysis closely mirrored what happened in reality and the differences between the measured deflections in the model and in the test was less than 0.1 mm. Only one loading scenario was where the difference was higher than modelled and this was where the load was positioned over the female joint. This was outlined in the AECOM report which determined very poor subgrade stiffness in this area. The results of the test and the FEA can be seen in Figure 44.

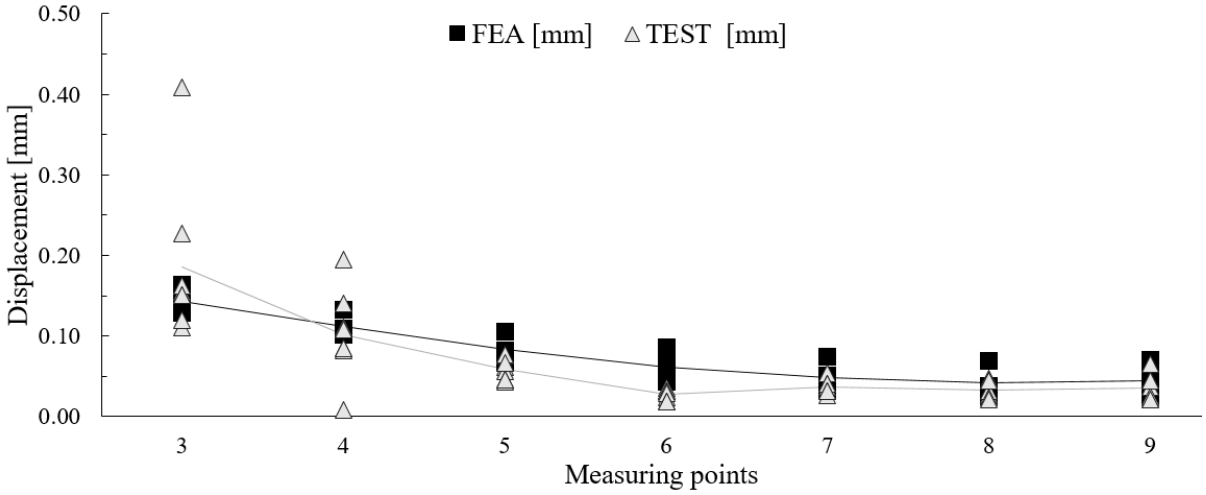

Figure 44: Results of RTST and FEA

8.8 Conclusion

The use of macro synthetic fibre reinforced concrete has become more and more popular in the building industry and thus also in the concrete track slab constructions. Track slab structures are typically heavily exposed to weather and mechanical loads, and because of this must have sufficient ductility and durability. At the same time the repair or replacement of these elements is difficult as generally the traffic must be stopped for a long periods during this process. Based on these criteria the use of macro synthetic fibre is a good alternative reinforcement to mesh and steel bars. The concrete reinforced with the already mixed in corrosion-free fibres is easy to handle and the track slab can be constructed faster,

thus by using FRC, labour can be decreased and the ductility increased. Further macro synthetic fibres are better for dynamic loads also, which is a significant advantage of this type of construction.

Design and optimizing of the track slab means the determining of the required thickness of the track slab and the macro synthetic fibre dosage for the varying load cases, such as ultimate and serviceability limit state, and fatigue. For these special tasks advanced finite element software is needed. The influence of the fibres could be taken into account by the modification of the fracture energy of the plain concrete. These design models have been validated by full scale laboratory tests.

9. Conclusions and Software Evaluation Summary

Reinforcing the concrete with steel or synthetic macro fibres became a widely and fully accepted method in the concrete industry, although there are only a few design standards or guidelines available for the engineers. The concrete is a quasi-brittle material, the ductility and behaviour after crack thereof could be developed with the help of added fibres. To model this the modification of the material parameter of fracture energy is a practical, simple and also accurate method. The material models given in the guidelines sometimes over- and sometimes underestimate the effects of the fibres, their use at finite element analysis does not provide a precise result. As a result in our work we used a different approach: the Modified Fracture Energy Method, with the help of this the added fracture energy (G_{Ff}) can be determined by inverse analysis. This added fracture energy is a fibre type and dosage specific parameter which can be determined from laboratory results.

There was a large number of tests made at the experimental laboratory of Czako Adolf Laboratory (Department of Mechanics, Materials & Structures, Budapest University of Technology), where the added fracture energy was determined by inverse analysis. At researches and designs for the industry these parameters and calculation method were used. The added fracture energy (G_{Ff}) can be easy to use even for engineers less familiar with designing of FRC, and at the same time the numerical results are very close to the real scale test results. The added fracture energy depends mostly on the type and dosage of the fibre, so the manufacturers of the fibre can determine it in laboratories, and the engineers are able to use this as an initial input parameter. In case of major or important investments this parameter can be determined from the actual in-situ concrete to clarify and validate the calculation. This inverse analysis can also be made with the help of ATENA.

Based on the experience gained from this large number of extensive projects the usability and reliability of the software are proven. As a result of several years of developmental work on ATENA, it has become a fairly reliable and robust FE software for analysing FRC.

10. References

[1] ACI 544.8R-16, 'Report on Indirect Method to Obtain Stress-Strain Response of Fiber-Reinforced Concrete (FRC)', ACI Committee 544, 2016.
[2] Bažant, Z.P. and Oh, B.H, 'Crack Band Theory for Fracture of Concrete', Materials and Structures 16 (RILEM, 1983) 155-177.
[3] Bergmeister, K., Novák, D., Pukl, R., Červenka, V., Structural assessment and reliability analysis for existing engineering structures, theoretical background, Structure and Infrastructure Engineering, Vol. 5, Issue 4, August 2009, pp. 267-275.
[4] Bertagnoli, G., Giordano L., Mancini, G., Safety format for the nonlinear analysis of concrete structures, STUDIES AND RESEARCHES –V.25, Politech. di Milano, (2004) Italy.
[5] Cervenka, J., Pappanikolaou, V., Three dimensional combined fracture-plastic material model for concrete. Int. J. of Plasticity, Vol. 24, 12, (2008) 2192-2220, ISSN 0749-6419, doi:10.1016/j.ijplas.2008.01.004.
[6] Cervenka, V., 'Simulating a response', Concrete Engineering International, Vol. 4, No. 4, 2002, pp. 45-49.
[7] Červenka, J., Janda, Z., Pálek, P., Schaul, P., Sajdlová, T., D2.1 Modelling Prototype Software, FibreLAB project report v. 3.0, 29.1. 2018
[8] Červenka, J., Sajdlová, T., D3.1 FRC Parameter Optimization Prototype Software, FibreLAB project report v. 2.0, 29.1. 2018.
[9] Cervenka, V., Global Safety Format for Nonlinear Calculation of Reinforced Concrete. Beton- und Stahlbetonbau 103, Special Edition, Ernst&Sohn, (2008) 37-42.
[10] Cervenka, V., Reliability-based non-linear analysis according to fib Model Code 2010, Structural Concrete, Journal of the *fib*, Vol. 14, March 2013, ISSN 1464-4177, (2013) 19-28, DOI: 10.1002/suco.201200022.
[11] Cervenka V., Cervenka J., Jendele L., ATENA Program Documentation, Part 1 Theory, Prague, (2017), Cervenka Consulting, www.cervenka.cz.
[12] CNR-DT 204/2006, 'Guide for the design and construction of fibre reinforced concrete structures', CNR - Advisory Comittee on Technical Recommendations for Construction, Rome, 2007.
[13] Consoft - software documentation (2015). Available at: http://bauwesen.htwk-leipzig.de/nc/de/fakultaet-bauwesen/personen/name/slowik/
[14] EN 14651, 'Test method for metallic fibered concrete - Measuring the flexural tensile strength (limit of proportionality (LOP), residual)', European Committee for Standardization, 2005.
[15] *fib* Model Code for Concrete Structures 2010. Wilhelm Ernst & Sohn, Berlin, Germany, (2013), ISBN 978-3-433-03061-5.
[16] Juhász, K. P., 'Modified fracture energy method for fibre reinforced concrete', Fibre Concrete 2013, Prague, Czech Republic, pp. 89-90, ISBN 978-80-01-05238-9.
[17] Juhász, K. P., 'Szintetikus szálerősítésű betonok hozzáadott törési energiája az adalékanyag függvényében', Építés - Építészettudomány, 43 (3-4), 2015, pp. 315-327, ISSN 0013-9661.
[18] Kolísko, J., Tichý, J., Kalný, M., Huňka, P., Hájek, P. & Trefil, V., Development of ultra-high performance concrete (UHPC) on the basis of raw materials available in the Czech Republic. In: *Betonové konstrukce 21. století: betony s přidanou hodnotou*. Praha: Beton TKS (2012).

[19] Kovács, G., Juhász K. P., Precast, prestressed grandstand of PFRC in stadium, Hungary. In: *Central European Congress on Concrete Engineering: Concrete Structures in Urban Areas*. Wroclaw, Polland, 2013.09.04-2013.09.06.

[20] Lehký, D., Keršner, Z. and Novák,D., 'Determination of statistical material parameters of concrete using fracture test and inverse analysis based on FraMePID-3PB tool', in Proc. of Reliable Engineering Computing - REC 2012, June 2012, Brno, Czech Republic, ISBN 978-80-214-4507-9, 261-270

[21] Novák D., Vořechovský M., Rusina R., Small-sample probabilistic assessment – software FREET, *Proc 9th Int. Conf. on Applications of Statistics and Probability in Civil Engineering – ICASP 9,* Rotterdam: Millpress, pp. 91-96.

[22] Richtlinie Faserbeton, Österreichische Bautechnik Vereinigung (ÖVB), Wien, 2008.

[23] Pukl, R., Sajdlová, T., Červenka, J., Červenka, V., Performance of Fibre Reinforced Concrete Structures – Modelling of Damage and Reliability, *Consec*, Italy, 2016.

[24] Pukl, R., Havlásek, P., Vítek, P., Vítek, J.L., Vokáč, M., Bouška, P., Hilar, M., Numerical and experimental investigation of structural members made from RC and SFRC, fib Symposium, Tel Aviv 2013, (2013) 241-244.

[25] Pukl, R., Sajdlová, T., Lehký, D., Novák, D. 2013. 'Multi-level optimization of input parameters for modeling of fibre reinforced concrete'. In: fib Symposium 2013 - Engineering a Concrete Future: Technology, Modeling & Construction, Tel-Aviv, Israel, 135-138, ISBN 978-965-92039-0-1.

[26] Sajdlová, T., Kabele, P., 'Numerical simulations of functionally graded fiber reinforced cementitious composite members', 10th fib International PhD Symposium in Civil Engineering, Quebec, Canada, 2014.

[27] Sajdlová, T., Pukl, R., 'Optimization of input parameters for material model of fibre reinforced concrete and application on the numerical simulation of tunnel lining', ACI-fib International Workshop FRC, Montreal, Canada, 2014.

[28] Sajdlová, T., Pukl, R., Juhász, K.P., Nagy, L., Schaul, P., 'Fibre reinforced concrete constitutive laws for numerical simulation', CCC, Tokaj, Hungary, 2017.

[29] Sajdlova, T., Pukl, R., Kabele, P., 'The Issue of Numerical Analysis of Fibre Reinforced Concrete Structures', Fibre Concrete 2015, September 10-11, Prague, Czech Republic, 2015.

[30] Stehlik, E., Cyron D., Prague Metro's return to TBMs. Tunnels & Tunnelling International, August 2012.

[31] Vandewalle, L. et al., 'RILEM TC162-TDF: 'Test and Design Methods for Steel Fibre Reinforced Concrete: bending test' (final recommendation)', Materials and Structures, Vol. 36, 2003, pp. 560-567.

Acknowledgements

This document was created within the Eurostars project FibreLAB E!10316. The financial support of the Eurostars program and national funding agencies in Czech Republic and Hungary are greatly appreciated.

The partners in the project are:

Cervenka Consulting s.r.o. . ..... CER
JKP Static Ltd..... JKP

This report owes to a collaborative effort of the above organizations.

More information

Public FibreLAB reports are available through:

FibreLAB public web site http://www.fibrelab.eu

Copyright